contribute to the generation of granulomas in which aggregated macrophages engulfed Mtb are surrounded by a cuff of lymphocytes, including the $CD4^+$ and $CD8^+$ T cells (5, 6).

Mycobacterium bovis bacillus Calmette–Guérin (BCG) is an attenuated strain of *M. bovis* established by Calmette and Guérin for vaccination against Mtb. BCG vaccination to children has been reported to be efficacious against infant tuberculosis, especially miliary tuberculosis and tuberculous meningitis (7–9). However, prophylactic effect of BCG against adult pulmonary tuberculosis is variable in that the efficacy has ranged from 0 to 80% (10–12). Therefore, a new vaccine effective against adult pulmonary tuberculosis is required.

Since mucosal tissues of respiratory tract show unique immunoregulatory mechanism (13), a new vaccine strategy would be required to induce efficient protective immunity in the Mtb-infected lung. However, it is not well understood how induction of T_h1 and Tc1 responses is regulated in the lung after Mtb infection. In tissues such as skin and muscle that are usually used to inoculate vaccines, dendritic cells (DC) capture the inoculated pathogens or antigens and migrate into draining lymph node (LN) to present the antigen to T cells to initiate immune response. In contrast, pulmonary immune response was initiated not only in the lung-draining LN but also in bronchus-associated lymphoid tissue (14). Although it has been reported that pulmonary immune response is regulated by alveolar macrophages and cytokines such as IL-10 and transforming growth factor (TGF)-β (13), their involvement in regulation of anti-mycobacterial T_h1 cells in mycobacteria-infected lung is not clearly understood.

Mtb Ag85B is known as a major Mtb antigen that induces T_h1 response. A 15-mer peptide (Peptide-25, P25) covering amino acid residues 240–254 of the Ag85B has been reported to be recognized by $CD4^+$ T cells in MHC class II H-$2A^b$-restricted manner and induced T_h1 T cells producing IFN-γ and IL-2 (15–17). A transgenic (Tg) mouse line that expresses functional TCR specific for the P25 epitope of Ag85B in an A^b-restricted manner (P25 TCR-Tg mice) has been established (18). The P25 TCR-Tg $CD4^+$ T cells were activated to proliferate in the lung-draining mediastinal lymph node (MLN) from day 14 of pulmonary Mtb infection (19). Kinetics analysis of mycobacterial antigen-specific T cells using another Tg mice expressing TCR specific for Mtb-derived ESAT6 antigen showed that the T cells are activated between 7 and 10 days after pulmonary Mtb infection, whereas T_h1 response was demonstrated in the lung 15 days after the infection (20). For all the results, kinetics of T_h1 induction was not compared between vaccine strain BCG and virulent Mtb and between subcutaneous (s.c.) and pulmonary infection routs.

By using the P25 TCR-Tg mice, we analyzed kinetics of induction of mycobacterial antigen-specific $CD4^+$ T_h1 T cells after Mtb or BCG infection in the lung and compared the kinetics with that induced by s.c. infection. Furthermore, regulatory mechanism of the mycobacterial antigen-specific T_h1 T-cell induction in the lung was analyzed in the Tg T-cell system.

Methods

Animals

The P25 TCR-Tg mice express Ag85B P25 epitope-specific H-$2A^b$-restricted TCR from $CD4^+$ T-cell clone BP1 under C57BL/6 background (18). B6 Ly5.1 mice were a kind gift of Dr Yasunobu Yoshikai (Kyushu University, Fukuoka, Japan). Mice were used at 8–12 weeks of age. To supply normal T-cell repertoire to the P25 TCR-Tg mice, each P25 TCR-Tg mouse was transferred with 5×10^7 spleen cells from naive B6 Ly5.1 mice 1 day before infection (Normal T-cell repertoire-supplied (N)-P25 TCR-Tg mice). Experiments were conducted according to the Institutional Ethical Guidelines for Animal Experiments and the Safety Guideline for Living Modified Organism Experiments of the University of the Ryukyus under approval of the Animal Experiments Safety and Ethics Committee and the Living Modified Organism Experiments Safety Committee of the University of the Ryukyus, respectively.

P25 TCR-Tg T cell-specific anti-idiotype mAb

B cells from rats immunized with BP1-derived TCR-expressing rat TG40 cells were fused with SP2/0 myeloma cells, and a B-cell hybridoma that react with $CD4^+$ T cells of the P25 TCR-Tg mice but not to other T cells was established as the producer of anti-idiotype mAb KN7.

Microorganisms

Mtb H37Rv strain was grown in Middlebrook 7H9 broth (BD, Sparks, MD, USA) with albumin-dextrose-catalase enrichment (BD) at 37°C for 3 weeks. Viable bacterial number was determined on 7H10 agar plates (BD) with oleic acid-albumin-dextrose-catalase (OADC) enrichment (BD). BCG Tokyo strain was purchased from Japan BCG (Kiyose, Japan). The bacteria were re-suspended in PBS before use. Mtb was infected s.c. into footpad or i.t. with 1×10^3 or 5×10^6 colony-forming unit (CFU) in 50 μl of PBS. BCG were infected s.c. into footpad or i.t. with 5×10^6 CFU in 50 μl of PBS. Bacterial number in infected organs was determined by plating serially diluted organ homogenates onto 7H10 agar plates with OADC enrichment.

Cell preparation

Single-cell suspensions were prepared from the lungs as described (21). Footpad-draining popliteal and inguinal lymph node (DLN), lung-draining MLN and spleens were suspended by passing through 30-mm stainless steel mesh. Adherent splenocytes of B6 Ly5.1 mice were collected after 90 min culture and used as antigen presenting cells (APC).

Bacterial burden and cytokine assay

Mice were infected with s.c. into footpad or i.t. with 5×10^6 CFU of Mtb or BCG, and the DLN, MLN and lung were removed 1, 2 and 4 weeks later, homogenized in distilled water and plated on 7H10 agar (BD) to determine bacterial number. The lung homogenates were also used to determine IFN-γ levels by ELISA (R&D systems, Minneapolis, MN, USA).

Cell culture

Cells were suspended in RPMI 1640 medium (Wako, Osaka, Japan) supplemented with 10% FBS (Equitech Bio, Kerrville, TX, USA), 100 U ml^{-1} of penicillin (Meiji,

Yokohama Japan) and 100 μg ml^{-1} of streptomycin (Meiji) at 5 × 10^6 cells per ml and cultured with 5 μg ml^{-1} purified protein derivative (PPD) of Mtb (Japan BCG), recombinant (r) Ag85B of BCG or P25 peptide (FQDAYNAAGGHNAVF) (Invitrogen, Carlsbad, CA, USA). rAg85B was produced from yeast *Pichia pastoris* as secretory protein by using pPIC9K expression vector (Invitrogen) containing the full-length Ag85B gene cloned from the genomic DNA of BCG Tokyo strain.

FACS analysis

To analyze surface molecules on freshly isolated cells, cells were stained with biotin-conjugated anti-P25 TCR idiotype (KN7), anti-CD4 (Caltag, Burlingame, CA, USA), anti-CD69 (Caltag), anti-CD3 (PharMingen, San Jose, CA, USA) and anti-TCRβ (PharMingen) mAb. Before surface staining, cells were treated with HBSS containing 5% of 2.4G2 anti-FcRγ hybridoma supernatant to block non-specific binding.

To detect IFN-γ$^+$ T cells, cells were cultured in the presence or absence of PPD for 24 h, at 37°C in 5% of CO_2 with breferdin A (Golgi Plug, BD) for the last 6 h. The cells were pretreated with anti-FcRγ mAb, surface stained with allophycocyanin-conjugated anti-CD4 and biotin-conjugated anti-P25 TCR idiotype KN7 mAb followed by streptavidin–PE, then permeabilized and fixed with Cytofix/Cytoperm Reagent (BD) according to the manufacturer's instructions. The fixed/permeabilized cells were stained with FITC-conjugated anti-IFN-γ mAb (eBioscience, San Diego, CA, USA).

To label proliferating cells *in vivo*, mice were given 5-bromo-2-deoxyuridine (BrdU; Sigma–Aldrich, St Louis, MI, USA) at 0.8 mg ml^{-1} in drinking water during the last 3 days before analysis (22, 23). To label proliferating cells *in vitro*, naive splenocytes from the P25 TCR-Tg mice were stimulated with antigen for 7 days at 37°C 5% CO_2, then re-stimulated for 48 h with the antigen and APC in the presence of 10 μM BrdU. The BrdU-labeled cells were detected using a BrdU Flow kit (BD) according to the manufacturer's instructions.

The stained cells were analyzed with the FACSCalibur flowcytometer (BD) and CellQuest software (BD).

Reverse transcription–PCR

Total RNA was extracted, reverse transcribed and amplified by PCR as described (21). The PCR product was electrophoresed on a 1.8% agarose gel and then was observed by Gel Documentation system (Bio-Rad, Hercules, CA, USA). To perform real-time PCR assay, the cDNA was amplified using the iCycler iQ and the amplification data were analyzed by the $2^{-\Delta\Delta CT}$ method using Real-Time PCR Optical System Software Version 3.0 (Bio-Rad) as described (21). The PCR primers used were as follows: *TGF-β* sense (5′-ATTCCTGGCGTTACCTTGG-3′), *Tgfβ* antisense (5′-CCTGTATTCCGTCTCCTTGG-3′); *Il10* sense (5′-AGGGAGATTATATTATATGATGGG-3′), *Il10* antisense (5′-TTTCTCACCTCTCTTAGG-3′); *Il4* sense (5′-CGAAGAACACCACAGAGACTGAGCT-3′), *Il4* antisense (5′-GACTCATTCATGGTGCAGCTTATCG-3′) and *Actβ* sense (5′-TGGAATCCTGTGGCATCCATGAAA-C-3′), *Actβ* antisense (5′-TAAAACGCAGCTCAGTAACAGTCCG-3′).

Neutralizing mAb

Anti-IL-10 (SXC-1) mAb and anti-TGF-β (1D11) mAb were purified from hybridoma culture supernatants and 400 μg of the mAb was i.v. injected as indicated.

Statistical analysis

To compare more than three groups, a Kruskal–Wallis test was used to analyze difference of mean ranks of the groups, followed by a post-hoc test when significant result was obtained using the Kruskal–Wallis test. All the statistical analyses were carried out using Statcel2 software (OMS, Tokorozawa, Japan). A P value of <0.05 was considered to indicate significant difference.

Results

Experimental design to detect mycobacterial antigen-*specific T_h1 T cells in the lung*

To confirm the specificity and detection sensitivity of the anti-idiotype mAb KN7 established against the P25 TCR-Tg T cells, splenocytes prepared from the P25 TCR-Tg mice were stained with the mAb KN7. The mAb stained ~90% of TCRβ$^+$ spleen T cells of the P25 TCR-Tg mice (Fig. 1A), whereas negligible fraction of spleen cells of the wild-type C57BL/6 mice was stained with the KN7 mAb (data not shown). In addition, the P25 TCR-Tg mice and wild-type C57BL/6 mice were found equally susceptible for Mtb infection and capable to produce IFN-γ in the lung 4 weeks after lung infection (Fig. 1B and C) or i.v. infection (data not shown) of Mtb, suggesting that the P25 TCR-Tg mice are not vulnerable to Mtb infection.

Although there is a report showing three amino acid substitutions within the P25 epitope of BCG Tokyo strain compared with that of Mtb H37Rv strain (24), BCG Pasteur strain (GenBank AM408590) is known to have the identical epitope sequence to that of Mtb H37Rv strain. Therefore, we decided to re-examine genomic DNA sequence of the Ag85B gene from BCG Tokyo strain, and we found that BCG Tokyo strain has identical P25 epitope sequence to that of Mtb H37Rv (data not shown). In *in vitro* culture, the naive P25 TCR-Tg CD4$^+$ T cells are activated and proliferated equally to the synthetic P25 peptide, BCG Tokyo strain-derived rAg85B, as well as to the PPD of Mtb that contains high amount of Ag85B (25) as determined by CD69 expression and BrdU incorporation (Fig. 1D). These data confirmed that the P25 TCR-Tg CD4$^+$ T cells can recognize P25 epitope of both Mtb and BCG origin. Therefore, we decided to use both Mtb and BCG Tokyo strain for *in vivo* infection experiments of the P25 TCR-Tg mice and evaluated *in vitro* T-cell response using PPD which contain Mtb-derived Ag85B to stimulate the P25 TCR-Tg CD4$^+$ T cells in the following experiments.

To determine kinetics of induction of mycobacterial antigen-specific T_h1-type CD4$^+$ T cells, we initially transferred naive P25 TCR-Tg T cells (Ly5.2$^+$) into wild-type C57BL/6 Ly5.1 mice and then i.t. infected the mice with Mtb. Although *in vivo* proliferation of the transferred P25 TCR-Tg CD4$^+$ T cells was demonstrated after pulmonary Mtb infection (19), we failed to stably detect IFN-γ production of the transferred

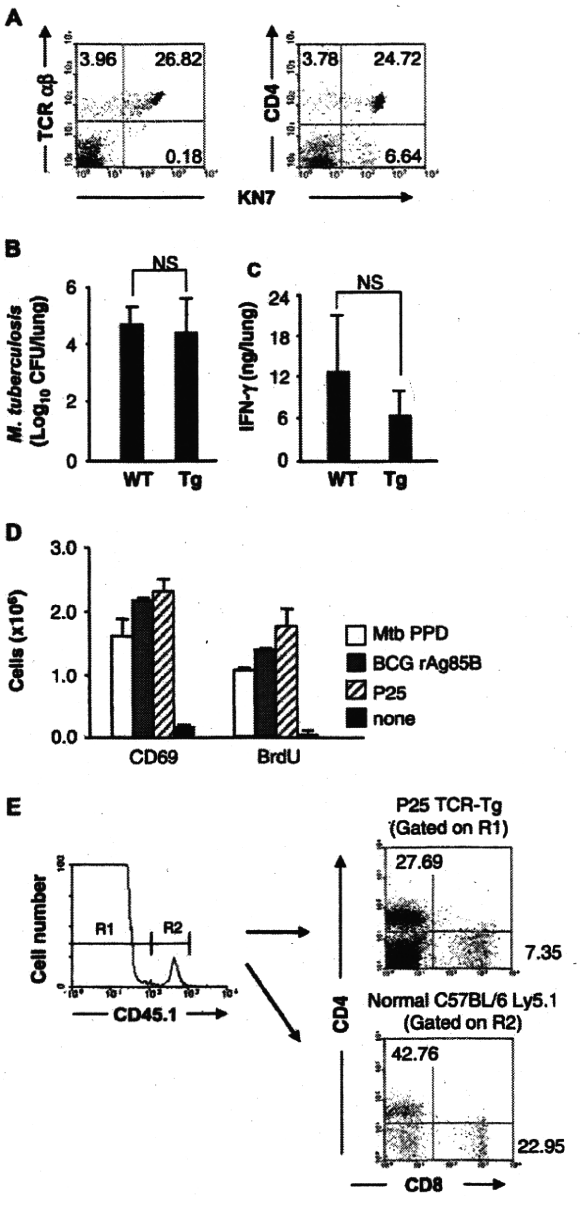

Fig. 1. Phenotype and anti-mycobacterial response of the P25 TCR-Tg mice. (A) Splenocytes from the naive P25 TCR-Tg mice were stained with anti-idiotypic mAb KN7, with anti-TCRβ or with anti-CD4 mAb. The cells were analyzed by FACS with analysis gate on lymphocytes. (B) Bacterial burden in the lungs of the wild-type or P25 TCR-Tg mice was analyzed 4 weeks after lung infection with 200 CFU of Mtb. The lungs were homogenized, plated on 7H10 agar and incubated to count the number of colonies. (C) IFN-γ levels in the lung homogenates were measured by ELISA 4 weeks after Mtb lung infection. (D) Activation and proliferation of the naive P25 TCR-Tg splenocytes were analyzed *in vitro*. Naive splenocytes from P25 TCR-Tg mice were cultured for 7 days with Mtb-derived PPD (open bars), BCG-derived rAg85B (gray bars), P25 peptide (striped bars) or without antigen (closed bars). Cells were re-stimulated for 48 h with relevant antigen, and the number of CD69-expressing and BrdU-incorporated P25 TCR-Tg CD4$^+$ T cells were measured by the FACS. The data shown are representatives of two independent experiments. (E) Detection of donor-derived CD45.1 cells in the lung of N-P25 TCR-Tg mice. Splenocytes of C57BL/6 Ly5.1 mice were intraperitoneal injection into P25 TCR-Tg mice. The next day, lymphocytes prepared from the lung were stained with anti-CD45.1 (Ly5.1), anti-CD4 and anti-CD8, and donor-derived CD45.1$^+$ T cells were detected by FACS. The data also demonstrate CD4 and CD8 expression of the donor-derived and the recipient P25 TCR-Tg mouse-derived T cells. The recipient-derived T cells are consisted of higher percentage of CD4$^+$ T cells which express Tg TCR, whereas donor-derived T cells showed normal CD4:CD8 ratio (~2:1).

P25 TCR-Tg CD4$^+$ T cells using KN7 mAb or anti-CD45.2 (Ly5.2) mAb in the mycobacteria-infected lung because the P25 TCR-Tg CD4$^+$ T cells are <1% of the total lung T cells even when 5×10^6 T cells were transferred, and IFN-γ$^+$ T cells represent <10% of the Tg CD4$^+$ T cells on day 28 after the infection (data not shown). Therefore, we concluded that a system which contains higher number of the P25 TCR-Tg CD4$^+$ T cells with normal T-cell regulatory system is required to analyze kinetics of mycobacterial antigen-specific T_h1-type T cells using the Tg mice. To overcome this problem, the P25 TCR-Tg mice were transferred with the normal T-cell repertoire of C57BL/6 Ly5.1 mice to construct the normal T cell-supplied (N)-P25 TCR-Tg mice. Twenty-four hours after the construction of the N-P25 TCR-Tg mice, the donor C57BL/6-Ly5.1-derived T cells were detectable with anti-CD45.1 mAb (Ly5.1) in the lung, (Fig. 1E). The N-P25 TCR-Tg mice were used to analyze the kinetics of activation and T_h1 differentiation of the P25 TCR-Tg CD4$^+$ T cells under normal immunoregulation after mycobacterial infection.

The Ag85B-specific P25 TCR-Tg CD4$^+$ T cells were activated and differentiated to T_h1 cells rapidly after BCG s.c. infection

Using the N-P25 TCR-Tg mice, we examined kinetics of bacterial number and activation, proliferation and T_h1 differentiation of the mycobacterial Ag85B-specific P25 TCR-Tg CD4$^+$ T cells after mycobacterial infection. We first analyzed the response of the P25 TCR-Tg CD4$^+$ T cells after s.c. infection of BCG into the footpads. After s.c. infection of 5×10^6 CFU of BCG, the bacteria was stably detected in the DLN until day 28 of the infection (Fig. 2A). The number of P25 TCR-Tg CD4$^+$ T cells in the DLN increased from day 3 and peaked on day 28 after the infection (Fig. 2B). The s.c. BCG infection induced expression of early T-cell activation marker CD69, proliferation detected by BrdU incorporation and IFN-γ expression of the P25 TCR-Tg CD4$^+$ T cells that are detected by FACS analysis (Fig. 2B). The IFN-γ expression was induced by antigen recognition of the P25 TCR-Tg CD4$^+$ T cells because IFN-γ production was not induced in the absence of *in vitro* antigen stimulation of the T cells (Fig. 2C). The number of the CD69$^+$ (Fig. 2D) and IFN-γ$^+$ (Fig. 2F) P25 TCR-Tg CD4$^+$ T cells peaked on day 3, and BrdU uptake of the T cells peaked on day 7 (Fig. 2E) after the s.c. BCG infection. Although the P25 TCR-Tg CD4$^+$ T cells showed the highest number on day 28 of the s.c. infection and IFN-γ$^+$ Tg CD4$^+$ T cell number also increased slightly on day 28, the increase was not statistically significant. Inoculation of low doses (1×10^3 to 1×10^4 CFU) of BCG failed to induce detectable activation and T_h1 induction

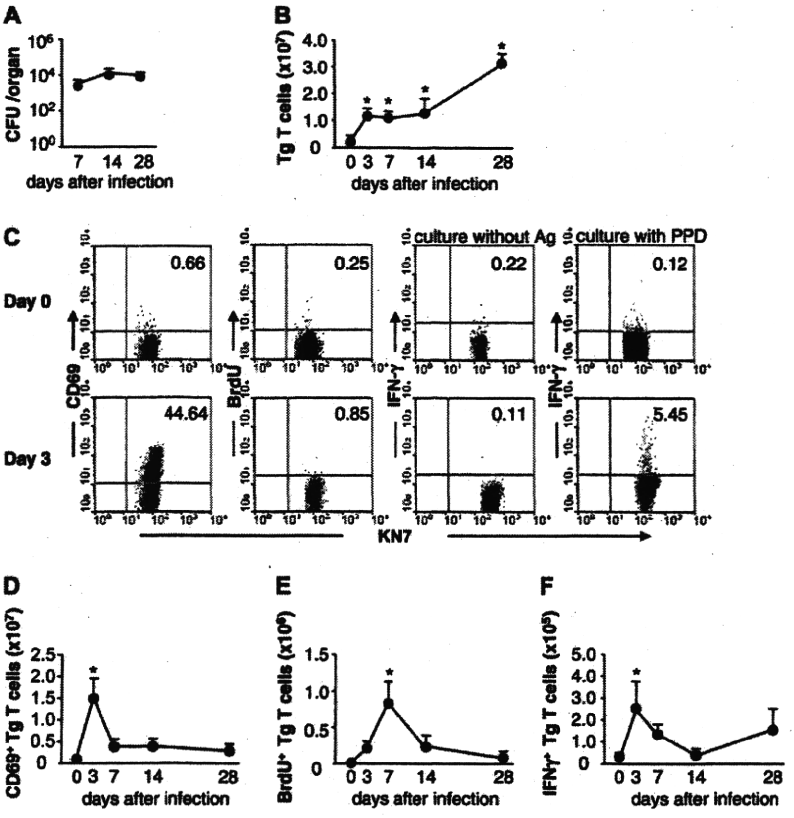

Fig. 2. Activation and T_h1 response of the P25 TCR-Tg CD4$^+$ T cells after BCG s.c. infection. The N-P25 TCR-Tg mice were s.c. infected with 5×10^6 CFU of BCG, and bacterial burden and the P25 TCR-Tg CD4$^+$ T cells in the DLN were analyzed. (A) Bacterial number in the DLN was analyzed on day 7, 14 and 28 after BCG s.c. infection. (B) The absolute number of the P25 TCR-Tg CD4$^+$ T cells detected as KN7$^+$ CD4$^+$ cells was measured on day 0, 3 and 7 after s.c. infection of BCG at the indicated doses. (C) FACS profile on the CD69 expression, BrdU incorporation or IFN-γ production of the P25 TCR-Tg CD4$^+$ T cells was analyzed in the DLN. Representative data on day 0, and 3 after s.c. infection of BCG are shown. Analysis gate was set on the P25 TCR-Tg CD4$^+$ T cells. (D–F) The absolute number of the CD69$^+$ (D), BrdU$^+$ (E) or IFN-γ$^+$ (F) P25 TCR-Tg CD4$^+$ T cells was measured on day 0, 3, 7, 14 and 28 after s.c. infection BCG. For data given in the panel (D–F), results are shown as mean ± SD, and the asterisks indicate significance of difference ($P < 0.05$) compared with the cell numbers on day 0. The data shown are as the representatives of two to five independent experiments with 3–5 mice used and individually analyzed for each experiment.

of the P25 TCR-Tg CD4$^+$ T cells at early stage of the infection (data not shown). These results suggest that the Ag85B-specific P25 TCR-Tg CD4$^+$ T cells in the DLN are activated and differentiated into T_h1 cells at early stage after s.c. BCG infection such as on day 3–7 when high dose (1–5 × 10^6 CFU) of BCG was infected.

The Ag85B-specific P25 TCR-Tg CD4$^+$ T cells were activated rapidly but differentiated to T_h1 cells at later stages in the lung and MLN after pulmonary BCG infection

We next analyzed kinetics of mycobacterial Ag85B-specific CD4$^+$ T-cell response after pulmonary BCG infection in the N-P25 TCR-Tg mouse system. We used high dose (5×10^6 CFU) of BCG in the pulmonary infection because the dose of BCG induced strong T-cell response while mice remained healthy after both s.c. and i.t. infection and maintained high bacterial burden in the lung and MLN until day 28 after the i.t. infection (Fig. 3A). After i.t. BCG infection, the P25 TCR-Tg CD4$^+$ T-cell number peaked on day 3 in the lung (Fig. 3B). In the MLN, the TCR-Tg T cell slightly increased on day 3 although the increase was not statistically significant (Fig. 3B). Representative FACS profiles of CD69 and IFN-γ expression of the P25 TCR-Tg CD4$^+$ T cells in the lung and MLN before and 28 days after BCG i.t. infection are shown in Fig. 3(C), and the kinetics of the CD69$^+$, BrdU$^+$ and IFN-γ$^+$ P25 TCR-Tg CD4$^+$ T cells are demonstrated in the Fig. 3(D–F). The data indicated that the CD69$^+$ and BrdU$^+$ P25 TCR-Tg CD4$^+$ T cells were vigorously increased (up to 270-folds) in the lung and MLN on day 3–7 of i.t. BCG infection followed by decrease of the number (Fig. 3D and E). In contrast, the T_h1-type IFN-γ$^+$ P25 TCR-Tg CD4$^+$ T cells were hardly detected on day 3 (Fig. 3F). Although low level of increase in the number of IFN-γ$^+$ P25 TCR-Tg CD4$^+$ T cells (<10-folds) was observed on day 7–21, there was no statistical significant increase when compared with that before i.t. BCG infection. Robust increase (20- to 30-folds) of the IFN-γ$^+$ P25 TCR-Tg CD4$^+$ T cells was seen on day 28 in the lung and MLN (Fig. 3F). These data indicate that

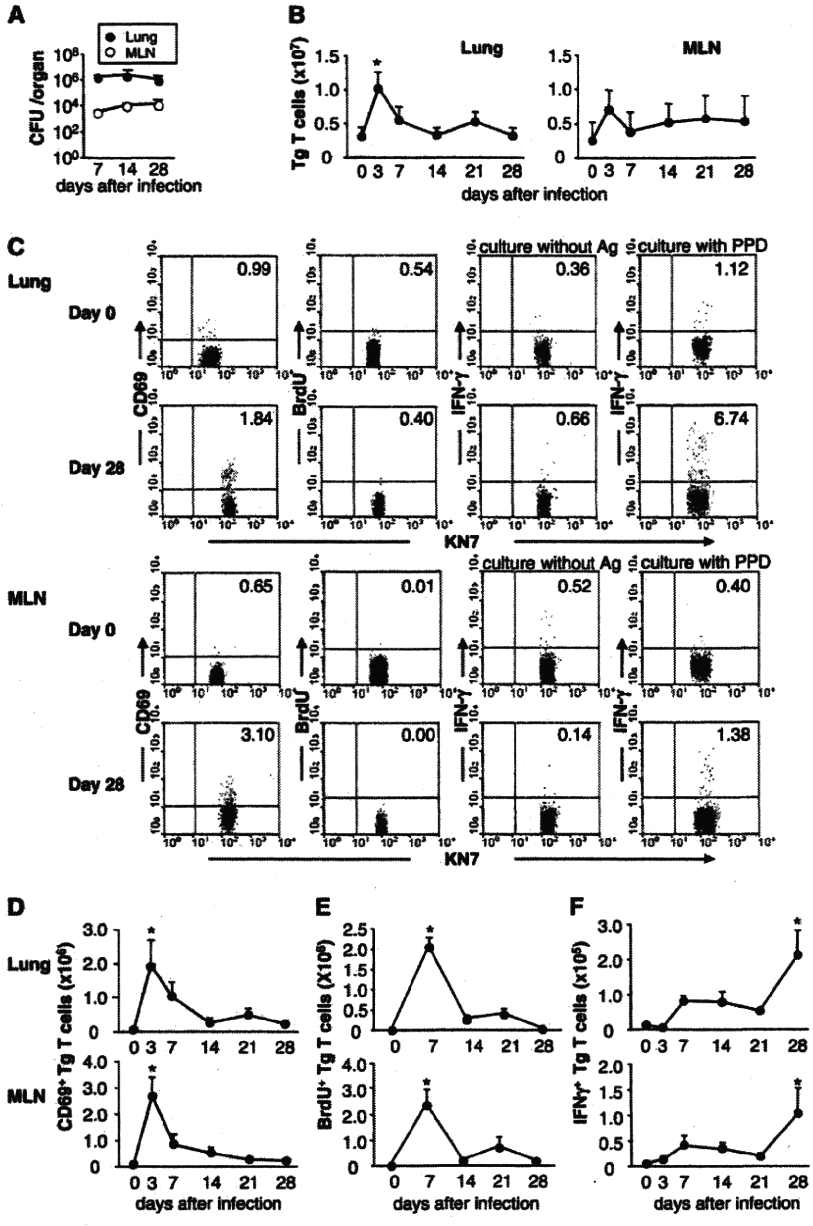

Fig. 3. Activation and T_h1 differentiation of the P25 TCR-Tg $CD4^+$ T cells after BCG lung infection. The N-P25 TCR-Tg mice were i.t. infected with 5×10^6 CFU of BCG, and the lung and MLN were analyzed. (A) Bacterial number in the lung and MLN was analyzed on day 7, 14 and 28 after BCG i.t. infection. (B) Kinetics of the absolute number of P25 TCR-Tg $CD4^+$ T cells in the lung and MLN after the infection. (C) Expression of the CD69 and IFN-γ in the lung and MLN determined on day 0 and 28 after i.t. infection. Analysis gate was set on P25 TCR-Tg $CD4^+$ T cells determined as $KN7^+$ $CD4^+$ cells. (D–F) The absolute number of $CD69^+$ (D), $BrdU^+$ (E) and IFN-γ^+ (F) P25 TCR-Tg $CD4^+$ T cells in the lung or MLN. Data in Fig. 3(A, B, D–F) are shown as mean ± SD, and the asterisks indicate significance of difference ($P < 0.05$) compared with the cell number on day 0. The data shown are as the representatives of two to five independent experiments with 3–5 mice used and individually analyzed for each experiment.

mycobacterial Ag85B-specific T_h1 response is fully established 3–4 weeks after activation and proliferation of the T cells in the lung and MLN of mice i.t. infected with high dose of BCG, whereas Ag85B-specific T_h1 response was induced in parallel to activation of the T cells after s.c. BCG infection. This suggests the presence of suppressive mechanisms against induction of T_h1 T-cell response in the lung.

Kinetics of activation and T_h1 differentiation of the P25 TCR-Tg CD4⁺ T cells after low-dose Mtb s.c. or i.t. infection

To analyze kinetics of activation and T_h1 induction of Ag85B-specific CD4⁺ T cells after Mtb infection and compare the responses with those seen in the BCG-infected mice, the N-P25 TCR-Tg mice were s.c. or i.t. infected with low dose (1×10^3 CFU) of Mtb. After the s.c. infection with low dose of Mtb, bacterial number was low on day 7, increased on day 14 and maintained the level until day 28 in the DLN (Fig. 4A). The P25 TCR-Tg CD4⁺ T-cell number slightly increased on day 3 and remarkably increased on day 28 in the DLN (Fig. 4B). The infection also induced significant increase of the CD69⁺ (Fig. 4C) and IFN-γ⁺ (Fig. 4E) P25 TCR-Tg CD4⁺ T cells on day 28 but not on day 3. BrdU⁺ proliferating P25 TCR-Tg CD4⁺ T cells showed no significant increase at the analyzed time points (Fig. 4D). Therefore, low-dose Mtb s.c. infection induced activation and T_h1 differentiation of the P25 TCR-Tg CD4⁺ T cells at a later stage of infection but not at an early stage of the infection.

Kinetics of mycobacterial Ag85B-specific CD4⁺ T-cell activation and differentiation in the lung and MLN was also analyzed after i.t. low-dose Mtb infection of the N-P25 TCR-Tg mice. Bacterial burden in the lung and MLN was low on day 7, increased on day 14 and maintained the level until day 28, as observed in the DLN of low-dose s.c. Mtb-infected mice (Fig. 5A). The cell number of total, CD69⁺ and IFN-γ⁺ P25 TCR-Tg CD4⁺ T cells showed significant increase in the lung on day 28 of the Mtb i.t. infection (Fig. 5B, C and F), whereas MLN showed significant increase of the CD69⁺ and IFN-γ⁺ P25 TCR-Tg CD4⁺ T cells on day 21 (Fig. 5C and E). Similar kinetics of induction of IFN-γ⁺ CD4⁺ T cells was observed in the wild-type C57BL/6 mice infected i.t. with low dose of Mtb (data not shown) and the mice infected with low-dose Mtb containing aerosol (19). Increase of the CD69⁺ T cells in the lung was not statistically significant on day 3. Induction of the BrdU⁺ P25 TCR-Tg CD4⁺ T cells was not observed even on day 28 after the infection (Fig. 5D). These data demonstrate that both activation and T_h1 differentiation of the mycobacterial Ag85B-specific CD4⁺ T cells became detectable 4 weeks and 3 weeks after low-dose Mtb i.t. infection in the lung and MLN, respectively, and the response may requires increase of bacterial burden in the infected organs. This is in consistent to the observation that proliferative response of the adoptively transferred P25 TCR-Tg CD4⁺ T cells was not detected until bacterial burden increased to $>1.5 \times 10^3$ CFU in MLN (19).

Early activation and T_h1 differentiation of the P25 TCR-Tg CD4⁺ T cells after high-dose Mtb s.c. or i.t. infection

Since low-dose BCG infection failed to induce early activation and T_h1 response of the P25 TCR-Tg CD4⁺ T cells, we estimated that low bacterial burden at an early stage of low-dose Mtb infection is a cause of the discrepancy between high-dose BCG infection and low-dose Mtb infection in induction of the response. To address the issue, we inoculated high dose (5×10^6 CFU) of Mtb and compared number of the CD69⁺ and IFN-γ⁺ P25 TCR-Tg CD4⁺ T cells between high dose-infected, low dose-infected and uninfected mice (Fig. 6). The analysis was carried out on day 3 after the infection because intratracheal infection of the high-dose Mtb is lethal but the infected mice survived for 4 to 5 days. The high-dose Mtb s.c.-infected mice showed significantly higher number of the P25 TCR-Tg CD4⁺ T cells expressing CD69 and IFN-γ in the DLN compared with the low-dose Mtb s.c.-infected or uninfected mice. In contrast, we detected no significant increase of the IFN-γ⁺ P25 TCR-Tg CD4⁺ T cells in the lung and MLN of the high-dose Mtb i.t.-infected mice compared with those in the low-dose Mtb i.t.-infected or uninfected mice although the CD69⁺ P25 TCR-Tg CD4⁺ T cells significantly increased in the lung by

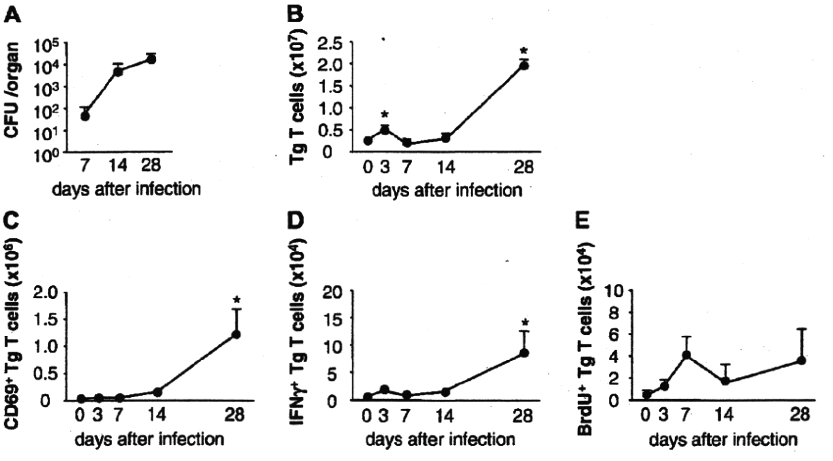

Fig. 4. Activation and T_h1 differentiation of the P25 TCR-Tg CD4⁺ T cells after low-dose Mtb s.c. infection. The N-P25 TCR-Tg mice were s.c. infected with 1×10^3 CFU of Mtb, and the DLN was analyzed (A). Bacterial number in the DLN was analyzed on day 7, 14 and 28 after Mtb s.c. infection. (B) Kinetics of the absolute number of the P25 TCR-Tg CD4⁺ T cells. (C–E) The absolute number of CD69⁺ (C), BrdU⁺ (D) and IFN-γ⁺ (E) P25 TCR-Tg CD4⁺ T cells in the DLN. Results are shown as mean ± SD, and the asterisks indicate significance of difference ($P < 0.05$) compared with the cell number on day 0. The data shown are representatives of two to five independent experiments with 3–5 mice individually analyzed for each experiment.

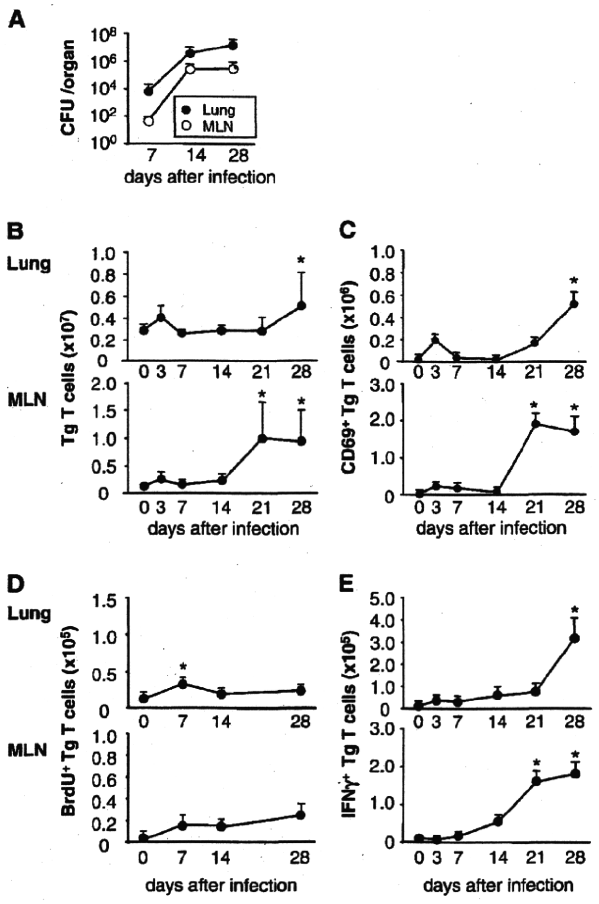

Fig. 5. Activation and T_h1 differentiation of the P25 TCR-Tg CD4$^+$ T cells after low-dose Mtb lung infection. The N-P25 TCR-Tg mice were i.t. infected with 1×10^3 CFU of Mtb, and the lung and MLN were analyzed. (A) Bacterial number in the lung and MLN was analyzed on day 7, 14 and 28 after Mtb i.t. infection. (B) Kinetics of the absolute number of the P25 TCR-Tg CD4$^+$ T cells in the lung and MLN. (C–E) Absolute number of the CD69$^+$ (C), BrdU$^+$ (D) and IFN-γ^+ (E) P25 TCR-Tg CD4$^+$ T cells in the lung and MLN. Results are shown as mean ± SD, and the asterisks indicate significance of difference ($P < 0.05$) compared with the cell number observed on day 0. The data shown are representatives of two to five independent experiments with 3–5 mice individually analyzed for each experiment.

the high-dose Mtb i.t. infection. The results suggest that early induction of T_h1-type immune response to Mtb is suppressed in the lung and MLN even in the presence of high dose of Mtb in the lung.

IL-10 partially suppressed induction of Mtb-specific T_h1 immune response in the lung

In low-dose Mtb i.t.-infected N-P25 TCR-Tg mice, IFN-γ^+ P25 TCR-Tg CD4$^+$ T cells were detected on day 21 after the infection but not in lung (Fig. 5). Since T_h2-type cytokines (IL-4 and IL-10) and TGF-β have been reported to suppress IFN-γ production (26), we next analyzed the possibility that the cytokines participate in the suppression of mycobacterial Ag85B-specific T_h1 response in the lung after mycobacterial infection. Reverse transcription (RT)–PCR analysis detected expression of *Il10* and *Tgfβ* but not *Il4* in the lung of naive and low-dose Mtb-infected mice (Fig. 7A). Real-time RT–PCR analysis showed enhancement of *Il10* and *Tgbβ* expression by Mtb i.t. infection (Fig. 7B), and therefore, we examined the influence of IL-10 and Tgfβ in the induction of T_h1 response in the lung of the Mtb-infected N-P25 TCR-Tg mice.

To address the possible involvement of IL-10 or TGF-β for suppression of T_h1 induction in the Mtb-infected lung, we examined the effects of the cytokine neutralization by anti-IL-10 or anti-TGF-β mAb treatment. The mAb were i.v. administered a day before Mtb i.t. infection to the N-P25 TCR-Tg mice. On day 14, 21 and 28 after the infection, the lung and MLN were analyzed for IFN-γ production. As shown in Fig. 7(C), anti-IL-10 mAb-treated mice showed significant increase in the number of the IFN-γ^+ P25 TCR-Tg CD4$^+$ T cells in the lung on day 21 but not on day 14 and 28 after the infection. IFN-γ^+ P25 TCR-Tg CD4$^+$ T cells in the MLN did not increased by the same mAb treatment. The kinetics of CD69 expression was not affected by the anti-IL-10 mAb treatment (data not shown). In contrast, anti-TGF-β mAb treatment showed no effect on the number of IFN-γ^+ P25 TCR-Tg CD4$^+$ T cells after Mtb infection (data not shown). Since it is possible that a single anti-TGF-β mAb treatment was not sufficient to fully neutralize the biological function of TGF-β, the anti-TGF-β mAb was repeatedly inoculated i.v. every week. However, it failed to accelerate induction of the IFN-γ^+ P25 TCR-Tg CD4$^+$ T cells (Fig. 6D). CD69 induction of the P25 TCR-Tg CD4$^+$ T cells was not influenced by the anti-TGF-β mAb treatment (data not shown). These data suggested that IL-10, but not TGF-β, is partially involved in the suppression of T_h1 induction after Mtb i.t. infection in the lung.

Discussion

In the present report, we analyzed kinetics of appearance of T_h1-type CD4$^+$ T cells in the lung of the mice with high number of naive TCR-Tg CD4$^+$ T cells specific for mycobacterial Ag85B (N-P25 TCR-Tg mice) after mycobacterial pulmonary infection. The results suggest that it requires 4 weeks after pulmonary infection of Mtb or BCG to fully establish mycobacterial antigen-specific T_h1 response in the lung and MLN, whereas it takes only a week to establish T_h1 response in DLN after s.c. infection of the mycobacteria. Therefore, we concluded that T_h1-type immune response is controlled in the mycobacteria-infected lung through lung-specific mechanisms which may include suppression of T_h1 induction as discussed below.

Our data showed that T_h1 induction of the Ag85B-specific P25 TCR-Tg CD4$^+$ T cells requires >3 weeks in the lung and MLN even when activated (CD69$^+$) or proliferated (BrdU$^+$) P25 TCR-Tg CD4$^+$ T cells increased quickly by day 3 after high-dose BCG or Mtb lung infection. From this observation, we speculated that antigen presentation to the P25 TCR-Tg CD4$^+$ T cells occurred in the MLN and the lung after high-dose lung mycobacterial infection but T_h1 induction was not induced at this stage. Wolf *et al.* (19, 27) reported using the P25 TCR-Tg CD4$^+$ T cell-transferred mice that lung DC

captured Mtb and migrated into the MLN on day 17 of low-dose aerosol Mtb infection and induced proliferative response of the P25 TCR-Tg CD4$^+$ T cells (19). They detected IFN-γ-producing P25 TCR-Tg CD4$^+$ T cells on day 17 in the lung and MLN in proliferating P25 TCR-Tg CD4$^+$ T cells (19). Gallegos *et al.* (20) also reported using another Tg mice expressing TCR derived from CD4$^+$ T cells specific for a major Mtb antigen ESAT-6 that adoptively transferred CD4$^+$ Tg T cells were activated in MLN on day 7–10 and differentiated into T_h1 T cells by day 15. Furthermore, Mittrücker *et al.* (28) demonstrated that pulmonary Mtb infection of normal mice induced mycobacterial Ag85A- and Ag85B-specific T_h1-type CD4$^+$ T cells in the lung on day 28 but not on day 14 of the infection. These data are consistent to our results in that induction of mycobacterial antigen-specific T_h1-type CD4$^+$ T cells was detected at relatively late stage of immune response after encounter with mycobacteria. Wolf *et al.* (27) attributed the delay of the appearance of mycobacterial antigen-specific T_h1 T cells to the delay of antigen presentation by DC. However, our data suggest that antigen presentation to the P25 TCR-Tg CD4$^+$ T cells occur at an early stage of high-dose BCG infection and induced T cell activation, but induction of IFN-γ production still requires >3 weeks. Therefore, not only delayed migration of antigen loaded DC into the MLN but also other immune regulatory mechanisms may be involved in the control of T_h1 response in the mycobacteria-infected lung.

Although bystander activation of T cells have been reported, we consider that the activation and IFN-γ production of the P25 TCR-Tg CD4$^+$ T cells in the N-P25 TCR-Tg mice were induced by TCR-mediated mycobacterial antigen recognition after mycobacterial infection. Bystander activation was reported in various infections *in vivo*, especially on CD8$^+$ T cells (29). However, there was only marginal IFN-γ production of the P25 TCR-Tg CD4$^+$ T cells when the cells were cultured without mycobacterial antigen, which suggest that the T cells recognize specific antigen to produce IFN-γ. Antigen-specific *in vivo* response of the P25 TCR-Tg CD4$^+$ T cells was also demonstrated by Wolf *et al.* (19). They demonstrated that infection of Ag85B-deficient Mtb failed to induce proliferation of adoptively transferred P25 TCR-Tg CD4$^+$ T cells *in vivo* although bacterial burden in the lung and MLN of the Ag85B-deficient Mtb-infected mice was nearly the same as that of mice infected with wild-type Mtb. CD69 expression could also be served as a hallmark of TCR-mediated T-cell activation. CD69 expression was induced in parallel to IFN-γ production in the P25 TCR-Tg T cells after s.c. BCG infection although the number of the IFN-γ$^+$ cells were less than that of the CD69$^+$ cells. In contrast, i.t. mycobacterial infection induced early CD69 expression without IFN-γ expression in the lung and MLN. All the observation suggest that the P25 TCR-Tg CD4$^+$ T cells are activated *in vivo* by antigen recognition after mycobacterial infection and express early T-cell activation marker CD69.

It is also intriguing that the CD69$^+$ and IFN-γ$^+$ P25 TCR-Tg CD4$^+$ T cells increased in the absence of detectable BrdU incorporation at later stage of low-dose Mtb infection. Although the mechanism is not yet clarified, there are several possibilities. First, it is possible that Mtb-infected DC deliver inefficient signals to the T cells which is enough to induce CD69 expression but not sufficient to induce strong clonal expansion. This is in consistent to the observation that total P25 TCR-Tg CD4$^+$ T-cell number in the lung and MLN marginally increased after the low-dose Mtb infection. Second, it is possible that the P25 TCR-Tg CD4$^+$ T cells proliferate transiently at a restricted time point after pulmonary Mtb infection. Wolf *et al.* (19) demonstrated that absolute number of the adoptively transferred P25 TCR-Tg CD4$^+$ T cells increased in the Mtb-infected lung and MLN on day 17 but not on day 14 or day 21. *In vivo* proliferation assay using carboxyfluorescein diacetate succimidyl ester-labeled cells also showed that the P25 TCR-Tg CD4$^+$ T cells proliferated on day 17 but not on day 14 after the Mtb infection, and the ratio of proliferated P25 TCR-Tg CD4$^+$ T cells seems to be nearly the same on day 21 compared with that on day 17 (19). All the data suggest the possibility that Mtb infection

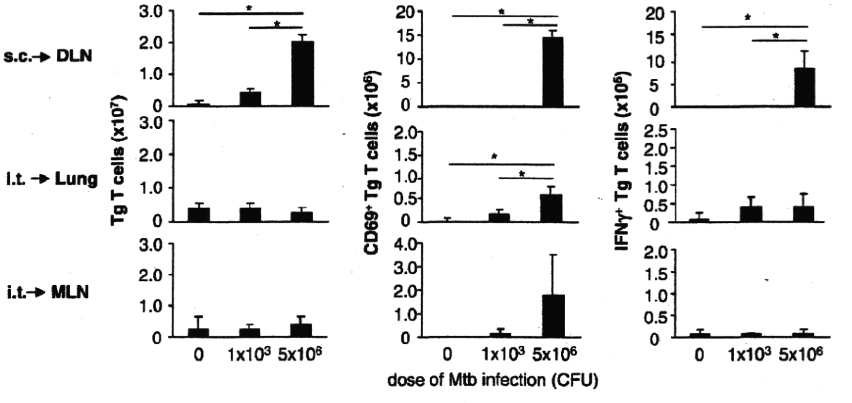

Fig. 6. Activation and T_h1 differentiation of the P25 TCR-Tg CD4$^+$ T cells at an early stage of high-dose Mtb infection. The N-P25 TCR-Tg mice were s.c. or i.t. infected with 1×10^3 CFU or 5×10^6 CFU of Mtb, and the DLN, lung and MLN were analyzed before or 3 days after the infection. Total number of P25 TCR-Tg CD4$^+$ T cells (left panels), and absolute number of CD69$^+$ (middle panels) or IFN-γ$^+$ (right panels) P25 TCR-Tg CD4$^+$ T cells in the DLN after s.c. Mtb infection or in the lung and MLN after i.t. Mtb infection are demonstrated. Results are shown as mean ± SD, and the asterisks indicate significance of difference ($P < 0.05$) compared with the cell number observed on each groups. The data shown are representatives of two independent experiments with 3–5 mice individually analyzed for each experiment.

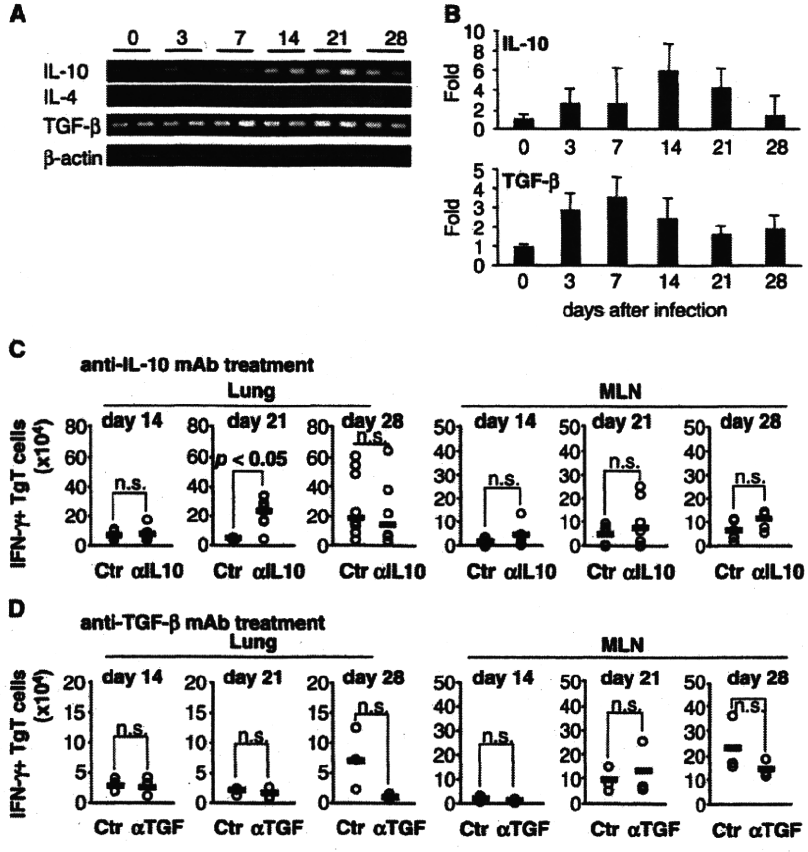

Fig. 7. Effects of regulatory cytokines on the induction of T_h1 response of the P25 TCR-Tg CD4$^+$ T cells after low-dose Mtb lung infection. (A) Transcripts for TGF-β, IL-10, IL-4 and β-actin in the Mtb-infected lung of the wild-type mice were analyzed by electrophoresis of RT-PCR products and ethidium bromide staining. (B) TGF-β and IL-10 mRNA expression levels in the Mtb-infected lung of the wild-type mice were analyzed by real-time RT-PCR with normalization using β-actin mRNA expression level. Expression levels on day 0 were arbitrarily set to 1.0. (C and D) The N-P25 TCR-Tg mice were injected i.v. with anti-IL-10 mAb (αIL10) a day before i.t. inoculation with 1×10^3 Mtb. Control group (Ctr) was left untreated with mAb. The IFN-γ$^+$ P25 TCR-Tg CD4$^+$ T cells in the lung and MLN were detected by FACS, and absolute number of the IFN-γ$^+$ T cells was plotted individually. (D) The N-P25 TCR-Tg mice were injected i.v. with anti-TGF-β mAb (αTGF) a day before and once a week after the i.t. inoculation with 1×10^3 CFU of Mtb. The IFN-γ$^+$ P25 TCR-Tg CD4$^+$ T cells in the lung and MLN were detected by FACS, and absolute number of the IFN-γ$^+$ T cells was plotted individually. n.s., not significantly different compared with the mAb-untreated group. The data shown are representatives of two independent (A and B) or three independent (C and D) experiments.

induced only transient proliferation of the P25 TCR-Tg CD4$^+$ T cells around day 17 post-infection although underlining mechanism of the transient proliferation is not yet clarified. In our analysis, BrdU incorporation was analyzed on day 7, 14, 21 and 28 after intratracheal Mtb infection, and the point of transient proliferation would not be included in the analysis.

Our data showed that anti-mycobacterial T_h1 response is not observed in the lung when mycobacterial antigen-specific T_h1 cells were detected in the MLN on day 21 of the low-dose Mtb infection. From this observation, we estimated that activated T_h1 cells are suppressed in the lung at this time point. A possible candidate mechanism of this suppression is suppressive cytokines such as IL-4, IL-10 and TGF-β which have been reported to suppress T_h1 response (26). RT-PCR analysis of the infected lung identified induction of IL-10 and TGF-β expression after the pulmonary Mtb infection. When the cytokines were neutralized with mAb, anti-IL-10 mAb resulted in increase of the IFN-γ-producing P25 TCR-Tg CD4$^+$ T cells in the lung on day 21 when T_h1 response was induced in the MLN but anti-TGF-β mAb had no effect on the induction. Therefore, we estimate that T_h1-committed T cells induced in the MLN around day 21 after Mtb infection may migrate into the infected lung but failed to be activated and expand because of IL-10-mediated produced in the Mtb-infected lung.

Regulatory T cell (Treg)-mediated suppression of lung T-cell response is another possible mechanism of suppression of T_h1 T cells in the mycobacteria-infected lung. Scott-Browne *et al.* (30) reported that FoxP3$^+$ Tregs increased in the lung after Mtb infection. Furthermore, depletion of the Treg resulted in enhanced protection in the lung, suggesting suppression of protective immunity against Mtb by Treg in the lung. Interestingly, T_h1 response to Mtb-derived ESAT-6 antigen paradoxically decreased in the Treg-depleted Mtb-infected mice (30), suggesting that Treg may not always suppress T_h1 induction in the mycobacteria-infected lung. In our Tg system,

naive P25 TCR-Tg mice without T-cell transfer contained very low level of FoxP3$^+$ T cells (0.3% of the lung T cells) and transfer of normal T-cell repertoire to prepare the N-P25 TCR-Tg mice resulted in >2-fold increase in the Treg in the lung. However, the P25 TCR-Tg mice and N-P25 TCR-Tg mice contained nearly the same number of IFN-γ-producing P25 TCR-Tg CD4$^+$ T cells on day 21 after Mtb lung infection (data not shown). The experiment did not support Treg-mediated suppression as a major suppressive factor of T_h1 development in the lung after mycobacterial infection.

Alternatively, it is possible that innately programmed pulmonary microenvironment suppress induction of T_h1 response, especially at an early stage of mycobacterial lung infection. It was reported that alveolar macrophages secreted nitric oxide, TGF-β and prostaglandin E_2 that control the function of DC (14, 31, 32). Furthermore, it has been reported that alveolar macrophages suppress maturation of lung DC to express MHC class II (31, 33), which may result in suppression of T_h1 response in the lung. Lung plasmacytoid DC were reported as immunomodulatory cells which shift immune response to T_h2 type (34). Pulmonary DC subpopulation was reported to suppress T_h1 response via IL-10 production (35). Interestingly, adoptive transfer of bone marrow-derived DC into the lung rapidly induced T-cell proliferative response and cytokine production including IFN-γ (36). The innately programmed suppressive mechanisms may suppress early stage of T_h1 immune response after mycobacterial lung infection. To address the hypothesis that pulmonary microenvironment constructed by alveolar macrophages suppress function of lung DC to induce T_h1 response, a preliminary experiment was carried out using mice depleted of pulmonary macrophages and DC and transferred systemically or intratracheally with bone marrow-derived DC before pulmonary BCG infection. Unexpectedly, the mice showed no accelerated induction of mycobacterial antigen-specific T-cell response in the lung. Therefore, alveolar macrophage-mediated suppression would not be an important mechanism of the delay in induction of T_h1 response in the lung. Further analysis on immunoregulatory function of pulmonary DC is on going.

Funding

Program of Founding Research Centers for Emerging and Reemerging Infectious Diseases, Ministry of Education, Culture, Sports, Science and Technology (MEXT) of Japan; Grant-in-Aids for Scientific Research, Japan Society for Promotion of Science.

Acknowledgements

We thank Dr Y. Yoshikai for providing B6 Ly5.1 mice.

Disclosures

The authors have no financial conflict of interest.

References

1 Dye, C., Floyd, K. and Uplekar, M. 2008. *Global Tuberculosis Control: Surveillance, Planning, Financing: WHO Report 2008.* World Health Organization, Geneva, Switzerland.
2 Cooper, A. M., Dalton, D. K., Stewart, T. A., Griffin, J. P., Russell, D. G. and Orme, I. M. 1993. Disseminated tuberculosis in interferon γ gene-disrupted mice. *J. Exp. Med.* 178:2243.
3 North, R. J. and Jung, Y. J. 2004. Immunity to tuberculosis. *Annu. Rev. Immunol.* 22:599.
4 Flynn, J. L. and Chan, J. 2001. Immunology of tuberculosis. *Annu. Rev. Immunol.* 19:93.
5 Kobayashi, K. and Yoshida, T. 1996. The immunopathogenesis of granulomatous inflammation induced by *Mycobacterium tuberculosis. Methods* 9:204.
6 Saunders, B. M. and Britton, W. J. 2007. Life and death in the granuloma: immunopathology of tuberculosis. *Immunol. Cell Biol.* 85:103.
7 Roche, P. W., Triccas, J. A. and Winter, N. 1995. BCG vaccination against tuberculosis: past disappointments and future hopes. *Trends Microbiol.* 3:397.
8 Hussey, G., Hawkridge, T. and Hanekom, W. 2007. Childhood tuberculosis: old and new vaccines. *Paediatr. Respir. Rev.* 8:148.
9 Walker, V., Selby, G. and Wacogne, I. 2006. Does neonatal BCG vaccination protect against tuberculosis meningitis? *Arch. Dis. Child.* 91:789.
10 Bloom, B. R. and Fine, P. E. M. 1994. The BCG experience: implications for future vaccines against tuberculosis. In Bloom, B. R., ed., *Tuberculosis: Pathogenesis, Protection and Control*, p. 531. ASM press, Washington, DC.
11 Editorial. 1980. BCG: bad news from India. *Lancet* 315:73.
12 Kristensen, I. and Jensen, H. A. P. 2000. Routine vaccinations and child survival: follow up study in Guinea-Bissau, West Africa. *BMJ* 321:1435.
13 Holt, P. G., Strickland, D. H., Wikström, M. E. and Jahnsen, F. L. 2008. Regulation of immunological homeostasis in the respiratory tract. *Nat. Rev. Immunol.* 8:142.
14 Moyron-Quiroz, J. E., Rangel-Moreno, J., Hartson, L. *et al.* 2004. Role of inducible bronchus associated lymphoid tissue (iBALT) in respiratory immunity. *Nat. Med.* 10:927.
15 Yanagisawa, S., Koike, M., Kariyone, A., Nagai, S. and Takatsu, K. 1997. Mapping of Vβ11+ helper T cell epitopes on mycobacterial antigen in mouse primed with *Mycobacterium tuberculosis. Int. Immunol.* 9:227.
16 Kariyone, A., Higuchi, K., Yamamoto, S. *et al.* 1999. Identification of amino acid residues of the T-cell epitope of *Mycobacterium tuberculosis* α antigen critical for Vβ11$^+$ Th1 cells. *Infect. Immun.* 67:4312.
17 Kariyone, A., Tamura, T., Kano, H. *et al.* 2003. Immunogenicity of peptide-25 of Ag85B in Th1 development: role of IFN-γ. *Int. Immunol.* 15:1183.
18 Tamura, T., Ariga, H., Kinashi, T. *et al.* 2004. The role of antigenic peptide in CD4$^+$ T helper phenotype development in a T cell receptor transgenic model. *Int. Immunol.* 16:1691.
19 Wolf, A. J., Desvignes, L., Linas, B. *et al.* 2008. Initiation of the adaptive immune response to *Mycobacterium tuberculosis* depends on antigen production in the local lymph node, not the lungs. *J. Exp. Med.* 205:105.
20 Gallegos, A. M., Pamer, E. G. and Glickman, M. S. 2008. Delayed protection by ESAT-6-specific effector CD4$^+$ T cells after airborne *M. tuberculosis* infection. *J. Exp. Med.* 205:2359.
21 Umemura, M., Yahagi, A., Hamada, S. *et al.* 2007. IL-17-mediated regulation of innate and acquired immune response against pulmonary *Mycobacterium bovis* bacille Calmette-Guerin infection. *J. Immunol.* 178:3786.
22 Mannering, S. I., Zhong, J. and Cheers, C. 2002. T-cell activation, proliferation and apoptosis in primary *Listeria monocytogenes* infection. *Immunology* 106:87.
23 Grujic, M., Christensen, J. P., Sørensen, M. R., Abrink, M., Pejler, G. and Thomsen, A. R. 2008. Delayed contraction of the CD8$^+$ T cell response toward lymphocytic choriomeningitis virus infection in mice lacking serglycin. *J. Immunol.* 181:1043.
24 Matsuo, K., Yamaguchi, R., Yamazaki, A., Tasaka, H. and Yamada, T. 1988. Cloning and expression of the *Mycobacterium bovis* BCG gene for extracellular alpha antigen. *J. Bacteriol.* 170:3847.
25 Wiker, H. G. and Harboe, M. 1992. The antigen 85 complex: a major secretion product of *Mycobacterium tuberculosis. Microbiol. Rev.* 56:648.

26 Sher, A., Gazzinelli, R. T., Oswald, I. P. *et al.* 1992. Role of T-cell derived cytokines in the downregulation of immune responses in parasitic and retroviral infection. *Immunol. Rev.* 127:183.
27 Wolf, A. J., Linas, B., Trevejo-Nuñez, G. J. *et al.* 2007. *Mycobacterium tuberculosis* infects dendritic cells with high frequency and impairs their function *in vivo*. *J. Immunol.* 179:2509.
28 Mittrücker, H.-W., Steinhoff, U., Köler, A. *et al.* 2007. Poor correlation between BCG vaccination-induced T cell responses and protection against tuberculosis. *Proc. Natl Acad. Sci. USA* 104:12434.
29 Gilbertson, B., Germano, S., Steele, P., Turner, S., Fazekas, G. B. and Cheers, C. 2004. Bystander activation of CD8+ T lymphocytes during experimental mycobacterial infection. *Infect. Immun.* 72:6884.
30 Scott-Browne, J. P., Shafiani, S., Tucker-Heard, G. *et al.* 2007. Expansion and function of Foxp3-expressing T regulatory cells during tuberculosis. *J. Exp. Med.* 204:2159.
31 Holt, P. G., Oliver, J., Bilyk, N. *et al.* 1993. Downregulation of the antigen presenting cell function(s) of pulmonary dendritic cells *in vivo* by resident alveolar macrophages. *J. Exp. Med.* 177:397.
32 Lipscomb, M. F., Pollard, A. M. and Yates, J. L. 1993. A role for TGF-beta in the suppression by murine bronchoalveolar cells of lung dendritic cell initiated immune responses. *Reg. Immunol.* 5:151.
33 Vermaelen, K. and Pauwels, R. 2005. Pulmonary dendritic cells. *Am. J. Respir. Crit. Care Med.* 172:530.
34 de Heer, H. J., Hammad, H., Soullié, T. *et al.* 2004. Essential role of lung plasmacytoid dendritic cells in preventing asthmatic reactions to harmless inhaled antigen. *J. Exp. Med.* 200:89.
35 Akbari, O., DeKruyff, R. H. and Umetsu, D. T. 2001. Pulmonary dendritic cells producing IL-10 mediate tolerance induced by respiratory exposure to antigen. *Nat. Immunol.* 2:725.
36 Lambrecht, B. N., Pauwels, R. A. and St Groth, B. F. 2000. Induction of rapid T cell activation, division, and recirculation by intratracheal injection of dendritic cells in a TCR transgenic model. *J. Immunol.* 164:2937.

CLINICAL AND VACCINE IMMUNOLOGY, Oct. 2010, p. 1500–1506 Vol. 17, No. 10
1556-6811/10/$12.00 doi:10.1128/CVI.00190-10

Influence of Advanced Age on *Mycobacterium bovis* BCG Vaccination in Guinea Pigs Aerogenically Infected with *Mycobacterium tuberculosis*▽

Shihoko Komine-Aizawa,[1,2]* Toshio Yamazaki,[3] Tsuyoshi Yamazaki,[4] Shin-ichiro Hattori,[1,5] Yuji Miyamoto,[6] Naoki Yamamoto,[1,7] Shinji Haga,[8] Masahiko Sugitani,[9] Mitsuo Honda,[1,2] Satoshi Hayakawa,[1,2] and Saburo Yamamoto[10]

AIDS Research Center,[1] Division of Biosafety Control and Research,[3] Department of Mycobacteriology, Leprosy Research Center,[6] and Department of Bacteriology,[8] National Institute of Infectious Diseases, Division of Microbiology[2] and Division of Pathology,[9] Department of Pathology and Microbiology, Nihon University School of Medicine, and Japan BCG Laboratory,[10] Tokyo, School of High-Technology for Human Welfare, Tokai University, Kanagawa,[4] and Division of Hematopoiesis, Center for AIDS Research, Kumamoto University, Kumamoto,[5] Japan, and Department of Microbiology, Yong Loo Lin School of Medicine, Singapore[7]

Received 10 May 2010/Returned for modification 1 June 2010/Accepted 26 July 2010

***Mycobacterium bovis* bacillus Calmette-Guérin (BCG) is the only tuberculosis (TB) vaccine currently available, but its efficacy against adult pulmonary TB remains controversial. BCG induces specific immune responses to mycobacterial antigens and may elicit protective immunity against TB. TB remains a major public health problem, especially among the elderly, yet the efficacy of BCG in the elderly is unknown. We investigated the ability of BCG vaccination to prevent TB in young (6-week-old), middle-aged (18-month-old), and old (60-month-old) guinea pigs. BCG-Tokyo vaccination reduced the growth of *Mycobacterium tuberculosis* H37Rv in all three groups. By use of an enzyme-linked immunospot (ELISPOT) assay, antigen-specific gamma interferon (IFN-γ)-producing cells were detected in the 60-month-old guinea pigs after a booster vaccination with BCG-Tokyo. Our findings suggest that BCG-Tokyo has a protective effect against tuberculosis infection regardless of age.**

Tuberculosis (TB) remains a major public health problem, especially among elderly people. Patients ≥60 years of age account for ≥50% of new cases in Japan (29). The increasing susceptibility of the elderly to *Mycobacterium tuberculosis* is generally thought to be associated with age-related changes in immune system function, especially losses or delays in antigen-specific $CD4^+$ T-cell function (14). Compromised antigen-specific $CD4^+$ T-cell responses may contribute to increased susceptibility to *M. tuberculosis* infection in mice (27).

Mycobacterium bovis bacillus Calmette-Guérin (BCG) is the only TB vaccine currently available. BCG has been used for more than 80 years (41), and vaccination with BCG is the standard for TB prevention in most countries. BCG induces specific immune responses to mycobacterial antigens and may elicit protective immunity against tuberculosis. BCG provides efficient protection against severe and disseminated TB, such as tuberculosis meningitis and miliary tuberculosis, in children (33, 34, 40). Although the long-term efficacy of BCG has been documented (3, 6), with several reports indicating efficient protection against disseminated TB in newborns and children, it appears to have less efficacy against adult pulmonary TB (2). In fact, its efficacy against pulmonary TB in both adults and the elderly is controversial, as is the efficacy of revaccination (5).

In the present study, we examined the efficacy of BCG against TB at different ages in a common guinea pig model (15, 25, 30). We used three age-segregated groups—young (6 weeks old), middle-aged (18 months old), and old (60 months old)—and we measured the number of antigen-specific gamma interferon (IFN-γ)-producing cells as an indicator of the efficacy of the vaccine against TB.

MATERIALS AND METHODS

Animals. Female pathogen-free outbred Hartley guinea pigs were purchased from Japan SLC (Shizuoka, Japan). The guinea pigs were divided into the three groups described above and were housed in accordance with the guidelines for animal experimentation of the Japanese Association for Laboratory Animal Science (1987) and in full compliance with the Law for the Humane Treatment and Management of Animals (Japan). The guinea pigs were fed and maintained in accordance with the guidelines set forth by the Institutional Animal Care and Use Committee of the National Institute of Infectious Diseases (NIID), Japan. Once approved by an institutional committee for animal experiments, these studies were conducted at the Animal Facility of Toyama Campus, NIID, Japan, in accordance with the requirements specifically stated in the Laboratory Biosafety Manual of the World Health Organization.

BCG vaccination. The guinea pigs were vaccinated with 5×10^5 CFU of BCG (strain Tokyo 172) injected subcutaneously into the left or right inguinal region. The vaccination schedules were as follows. The old guinea pigs were vaccinated with BCG, maintained for 60 months, and then revaccinated with BCG 6 weeks before *M. tuberculosis* infection (group 1; *n*, 2). The middle-aged guinea pigs were vaccinated either 18 months or 6 weeks before the infection (groups 2 and

* Corresponding author. Mailing address: Division of Microbiology, Department of Pathology and Microbiology, Nihon University School of Medicine, 30-1 Oyaguchi-Kamicho, Itabash-ku, Tokyo, Japan. Phone: 81-3-3972-8111. Fax: 81-3-3972-9560. E-mail: ashiho@med.nihon-u.ac.jp.

▽ Published ahead of print on 4 August 2010.

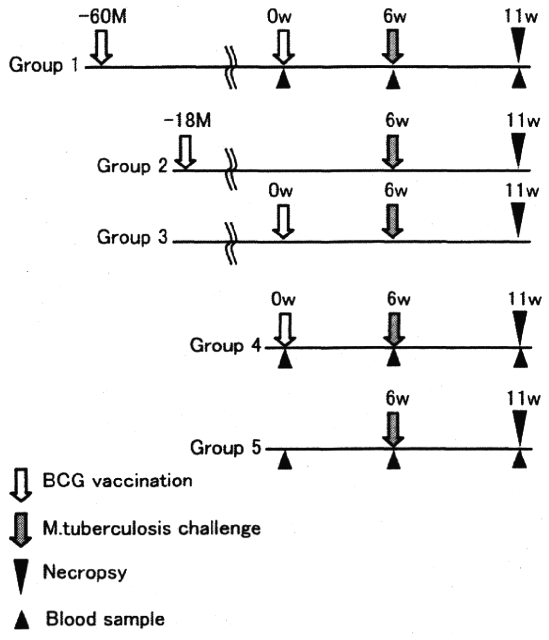

FIG. 1. Experimental design. Guinea pigs in the old group were vaccinated with BCG at the age of 6 weeks and were then maintained for 60 months before revaccination with BCG 6 weeks before *M. tuberculosis* infection (group 1). Guinea pigs in the middle-aged groups either were vaccinated with BCG at the age of 6 weeks and were then maintained for 18 months before infection (group 2) or were not vaccinated with BCG until 6 weeks before infection (group 3). Guinea pigs in the young groups either were vaccinated 6 weeks before infection (group 4) or were not vaccinated (group 5).

3, respectively; *n*, 3). The young animals either were vaccinated 6 weeks before the infection (group 4; *n*, 3) or were not vaccinated (group 5; *n*, 4) (Fig. 1).

Aerosol challenge with *M. tuberculosis* H37Rv. Virulent *M. tuberculosis* H37Rv (NIHJ1633) was grown in Middlebrook 7H9 broth (Difco, Detroit, MI) supplemented with albumin dextrose catalase (ADC) enrichment and 0.05% Tween 80 for 14 to 21 days at 37°C. The bacilli were subjected to gentle sonication in order to obtain a single-cell suspension and were frozen at −80°C until use. Thawed aliquots were diluted in phosphate-buffered saline (PBS) containing 0.05% Tween 20 to the desired inoculum concentration. BCG-vaccinated and unvaccinated guinea pigs were exposed to 2.5 ml of *M. tuberculosis* H37Rv at 5×10^4 CFU/ml by using an inhalation exposure system, model 4212 (Glas-Col, Terre Haute, IN). Then BCG-vaccinated and unvaccinated guinea pigs were infected with approximately 10 CFU of virulent *M. tuberculosis* H37Rv via the respiratory route. The animals were housed under biosafety level 3 conditions in a manner consistent with the international animal care and use guidelines of the National Institute of Infectious Diseases of Japan.

DTH skin test. To investigate delayed-type hypersensitivity (DTH) skin reactions, 0.2 μg of tuberculin purified protein derivative (PPD) was injected intradermally into BCG-vaccinated and unvaccinated guinea pigs, and the skin reactions were measured after 24 h.

Microbial enumeration. At 5 weeks postchallenge, specimens from the lungs, tracheal lymph node, and spleen from each (BCG-vaccinated or unvaccinated) aerosol-challenged guinea pig were removed aseptically and were homogenized separately in 1 ml of sterile saline using a Stomacher-80T instrument (Organo, Tokyo, Japan). Appropriate dilutions were inoculated onto 1% Ogawa medium (Kyokuto, Tokyo, Japan) and were incubated at 37°C for 3 weeks. The number of *M. tuberculosis* H37Rv colonies on the medium was counted and expressed as the mean $\log_{10}$ CFU per tissue.

Histopathology. The dissected lung samples from each guinea pig were fixed with 10% neutral-buffered formalin and were embedded in paraffin wax. The sections from these tissues were 4 μm thick and were stained with hematoxylin and eosin (H&E) or with Ziehl-Neelsen stain for acid-fast bacilli.

Preparation of cells. Mononuclear cells were isolated from the peripheral blood of the guinea pigs. Approximately 10 ml of blood was harvested from the animals by cardiac puncture at 0, 6, and 11 weeks after BCG vaccination. Before blood collection, the animals were anesthetized with ketamine (44 mg/kg). Peripheral blood mononuclear cells (PBMCs) were prepared with Lymphosepar (IBL Co., Ltd., Gunma, Japan) and were then adjusted to 1×10^6/ml in complete medium (RPMI 1640 supplemented with 10% fetal bovine serum). Cell viability was determined by a trypan blue dye exclusion test. Single-cell suspensions were cultured with or without PPD (10 μg/ml) at 37°C in a humidified 5% CO_2 environment for 40 h. Phytohemagglutinin (PHA) (1 μg/ml) was used as a positive control to stimulate whole T cells.

IFN-γ ELISPOT assay. IFN-γ-secreting cells were assessed by an enzyme-linked immunospot (ELISPOT) assay that was modified and improved to detect guinea pig IFN-γ-producing cells. Due to the low cross-reactivity of murine, rat, and guinea pig IFN-γ, we obtained a novel rabbit polyclonal anti-guinea pig IFN-γ antibody and developed a guinea pig IFN-γ ELISPOT assay system. Briefly, based on the predicted amino acid sequence of guinea pig IFN-γ described previously(16), we synthesized peptides (GG-1, GG-2, GG-3, GG-4, and GG-5). The immunogen (100 mg of peptide) was injected subcutaneously into rabbits, and 7 weeks after immunization, the rabbits were bled from the ear artery (50 to 100 ml). Antibodies were purified from antisera by affinity chromatography with immobilized synthetic peptides. Immunoblot analysis showed that only antisera against GG-2 and GG-5 reacted with a protein band of about 20 kDa, which is the putative molecular mass of guinea pig IFN-γ. Furthermore, the binding affinities of the purified antibodies for recombinant guinea pig IFN-γ were assessed. Recombinant guinea pig IFN-γ was prepared using the baculovirus system. Guinea pig IFN-γ cDNA was transfected into a baculovirus genome (Abv baculovirus; Katakura Industries Co. Ltd., Tokyo, Japan) with the pYNG transfer vector. Recombinant guinea pig IFN-γ was purified from the culture supernatant by an immunoaffinity column, and its bioactivity was measured based on the inhibition of the cytopathic effect of encephalomyocarditis virus (EMCV) on 104C1 guinea pig fibroblasts. We modified a previously described IFN-γ ELISPOT assay protocol (18) to detect guinea pig IFN-γ-producing cells. A polyclonal rabbit antibody to a guinea pig IFN-γ peptide was allowed to adhere overnight at 4°C to a 96-well nitrocellulose plate (MultiScreen-HA; Millipore, Billerica, MA) at a concentration of 5 μg/ml. The plate was washed with PBS–0.05% Tween 20 (PBST) and was then blocked with PBS supplemented with 1% bovine serum albumin (BSA) for 2 h at room temperature. Guinea pig PBMCs were transferred to the antibody-coated 96-well nitrocellulose plate in triplicate at an input cell number of 1×10^5 per well and were then incubated for 5 h at 37°C in a humidified 5% CO_2 environment. After 5 h of culturing, the plate was washed with PBST to remove cells and was then incubated with a biotinylated rabbit anti-IFN-γ secondary antibody at a concentration of 5 μg/ml for 2 h at room temperature. After a wash with PBST, the plate was treated with streptavidin-alkaline phosphatase and the substrate 5-bromo-4-chloro-3-indolylphosphate (BCIP)-nitroblue tetrazolium (NBT) (ELISPOT blue color module; R&D Systems, Minneapolis, MN). Spot-forming cells (SFCs) were quantified using the KS ELISPOT compact system (Carl Zeiss Japan, Tokyo, Japan).

Statistical analysis. The data were analyzed using the Tukey-Kramer test and Pearson's correlation coefficient test using Statcel 2 software. Differences between treatments were determined by the least-squares significant-difference multiple-comparison method. A probability level of 5% (P, <0.05) was considered statistically significant.

RESULTS

DTH skin responses of guinea pigs to PPD. DTH was assessed on the skin of guinea pigs 6 or 11 weeks after BCG inoculation both before and after challenge with *M. tuberculosis*. At week 6, significant DTH responses to PPD were detected in all of the guinea pigs vaccinated with BCG, while no response to PPD was detected in unvaccinated guinea pigs. The mean diameters of the indurations were as follows: 17.0 ± 4.2 mm (group 1), 20.0 ± 0.6 mm (group 2), 18.0 ± 1.7 mm (group 3), 15.3 ± 2.1 mm (group 4), and 5.5 ± 1.3 mm (group 5). No significant difference was observed among the groups vaccinated with BCG. DTH responses were detected in all groups at 5 weeks after the challenge with *M. tuberculosis* (Fig. 2).

BCG-induced PPD-specific T-cell responses. We examined the stimulation by PPD of IFN-γ production by the PBMCs of

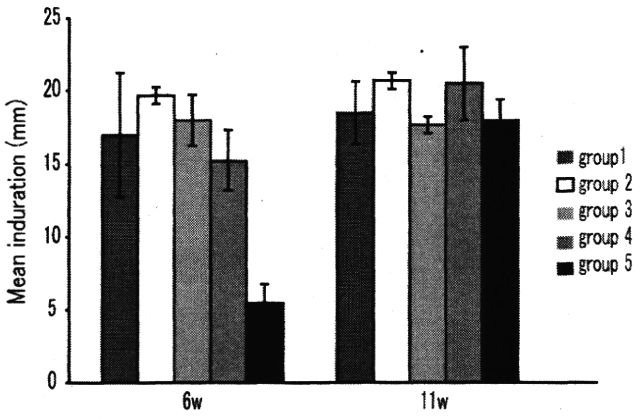

FIG. 2. PPD skin reactions of the guinea pigs. DTH was assessed on the basis of the skin reactions of guinea pigs 6 or 11 weeks (6w or 11w) after BCG inoculation both before and after challenge with *M. tuberculosis*. Error bars represent standard deviations. No significant difference among the groups vaccinated with BCG was observed.

the guinea pigs. To investigate T-cell functions specific for PPD, an IFN-γ ELISPOT assay was performed for groups 1, 4, and 5. The old guinea pigs of group 1 were inoculated with BCG 60 months before the infection and at week zero, and the young guinea pigs of group 4 were inoculated with BCG at week zero. Another group of young guinea pigs, group 5, was not inoculated. IFN-γ production by PBMCs was examined in each group at weeks zero, 6, and 11. At week 6 after the BCG vaccination, significant and specific IFN-γ responses to PPD were detected in groups 1 and 4 (Fig. 3). The mean numbers of SFCs among the PBMCs from the animals in groups 1 and 4 were 216.25 ± 24.50 and 108.75 ± 9.57, respectively. No significant IFN-γ production was detected in group 5. PPD-specific IFN-γ-secreting cells were more frequent among the PBMCs from group 1 than among those from group 4. Five weeks after the challenge with *M. tuberculosis* (at week 11 after the BCG vaccination), a significant increase in IFN-γ production by PBMCs following stimulation with PPD was observed in groups 1 and 4, although there was no difference between the groups in the mean frequency of cells responding specifically to PPD. The number of SFCs was also higher in group 5 after the challenge with *M. tuberculosis*. However, the number of SFCs was significantly lower than those in the BCG-vaccinated groups (P, < 0.01). At week zero of BCG vaccination, no increase in IFN-γ production was detected by the ELISPOT assay in group 1 in spite of the early BCG vaccination; groups 4 and 5 also showed no increase.

Effect of BCG vaccination on bacterial growth in young, middle-aged, and old guinea pigs challenged with *M. tuberculosis* H37Rv. To determine the impact of BCG vaccination on bacterial growth in young, middle-aged, and old guinea pigs, bacterial replication in the lungs (Fig. 4A), tracheal lymph nodes (Fig. 4B), and spleen (Fig. 4C) was examined for each group. In all cases, those animals vaccinated with BCG showed less bacterial growth in the lungs and tracheal lymph nodes than unvaccinated animals. In the spleen, no bacterial replication was detected except in groups 2 and 5. In group 2, which received BCG vaccination 18 months before the *M. tuberculosis* challenge, the effect of BCG may have been attenuated. Group

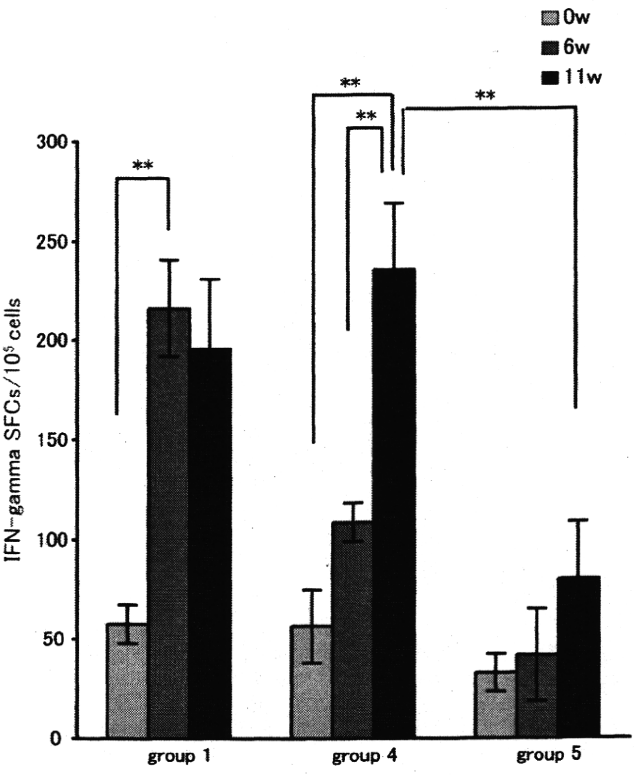

FIG. 3. BCG-induced PPD-specific T-cell responses. To investigate T-cell functions specific for PPD in groups 1, 4, and 5, an IFN-γ ELISPOT assay was performed at weeks zero, 6, and 11 after BCG vaccination. Error bars represent standard deviations. Asterisks indicate that the mean numbers of IFN-γ SFCs were significantly different. **, $P < 0.01$, as determined by analysis of variance (ANOVA) followed by a posthoc Tukey-Kramer test. There was no difference in IFN-γ SFCs between the old and young guinea pigs vaccinated with BCG.

1, which was revaccinated with BCG before the challenge, showed significantly less bacterial growth in the lungs than the unvaccinated guinea pigs (P, <0.05). In the tracheal lymph nodes, bacterial growth was also reduced, but the difference was not significant. We also found a significant negative correlation between the number of IFN-γ SFCs and the residual number of bacteria in the lungs (expressed in $\log_{10}$ CFU) 5 weeks after *M. tuberculosis* challenge (r, -0.6696; P, 0.04852) in groups 1, 4, and 5 (Fig. 5). This finding suggests that PPD-specific T-cell responses induced by BCG are crucial for the host defense against *M. tuberculosis* infection. Thus, BCG appears to have a protective effect in guinea pigs at all ages.

Histopathology. Figure 6 shows histopathological images of the lungs of young unvaccinated guinea pigs (Fig. 6a and b) and BCG-vaccinated guinea pigs (Fig. 6c and d) 5 weeks after *M. tuberculosis* challenge. Figure 6c shows a lung from a young BCG-vaccinated guinea pig (group 4), and Fig. 6d shows a lung from an old BCG-revaccinated guinea pig (group 1). In the lungs from unvaccinated guinea pigs, large granuloma nodules with central necrosis were predominant and consisted of epithelioid cells. Acid-fast bacilli were detected in the granulomas by Ziehl-Neelsen staining (Fig. 6b). Although granuloma nodules were also observed in the lungs of vaccinated guinea pigs

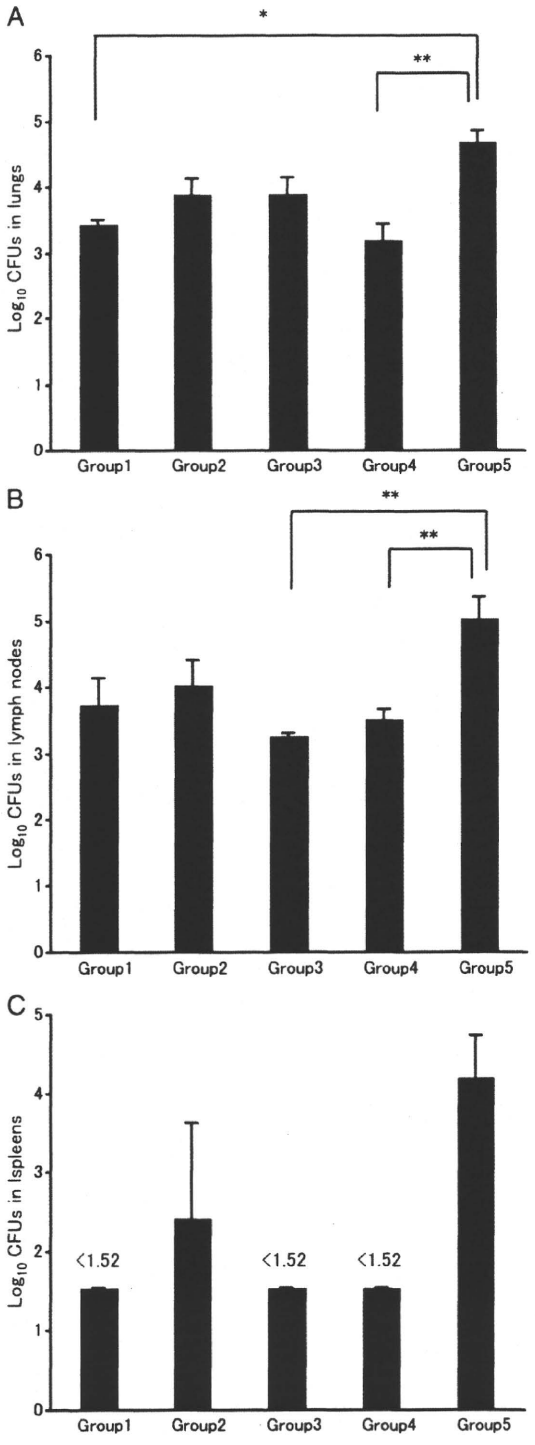

FIG. 4. Effects of BCG vaccination on bacterial growth in young, middle-aged, and old guinea pigs challenged with *M. tuberculosis* H37Rv. To determine the impact of BCG vaccination on bacterial growth, bacterial replication in lung (A), tracheal lymph node (B), and spleen (C) specimens from each guinea pig was examined. The minimum detectable level of bacilli in the tissue homogenate was 1.52 $\log_{10}$ CFU. Error bars represent standard deviations. Asterisks indicate that the mean numbers of *M. tuberculosis* CFU in an organ were significantly different. *, $P < 0.05$, and **, $P < 0.01$, as determined by analysis of variance (ANOVA) followed by a posthoc Tukey-Kramer test.

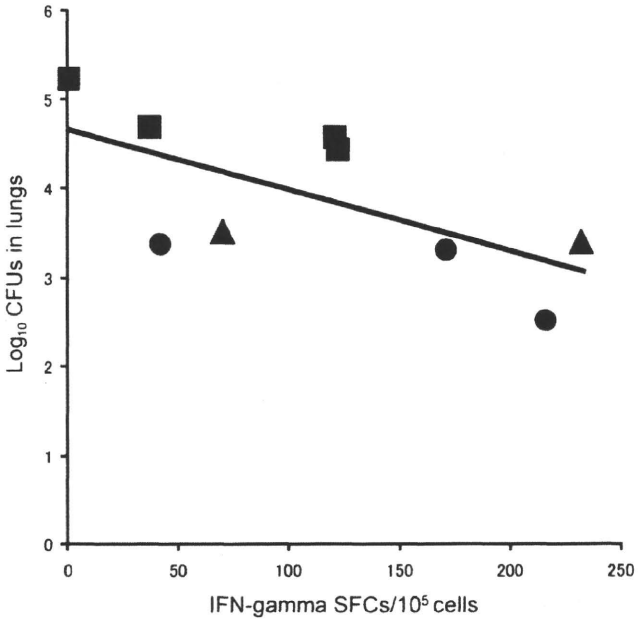

FIG. 5. Correlation between IFN-γ production and bacterial growth in the lungs. There was a statistically significant negative correlation between the number of IFN-γ SFCs detected 5 weeks after *M. tuberculosis* challenge and bacterial growth in the lungs (r, −0.6696; P, 0.04852 as determined by Pearson's correlation coefficient test). Circles, group 4 (young, vaccinated); squares, group 5 (young, unvaccinated); triangles: group 1 (old, revaccinated).

(Fig. 6c and d), vaccination with BCG reduced granuloma nodule formation in the lungs of both young and old guinea pigs, and no acid-fast bacilli were detected in the granulomas by Ziehl-Neelsen staining (data not shown).

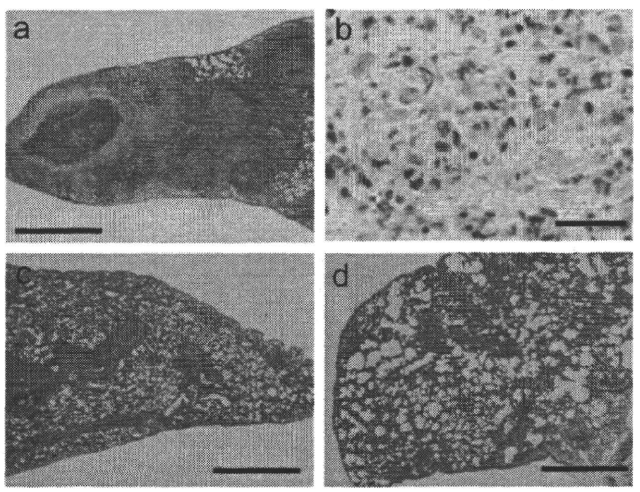

FIG. 6. Histopathology of lungs from guinea pigs infected with *M. tuberculosis* H37Rv. Shown are histopathological observations in the lungs of young unvaccinated (a and b), young BCG-vaccinated (c), and old BCG-revaccinated (d) guinea pigs 5 weeks after *M. tuberculosis* challenge. Bars, 1 mm (a, c, and d) and 50 μm (b).

DISCUSSION

BCG is the only TB vaccine currently available, and it has been used since 1921. It is inexpensive and safe, with few complications reported in infants. BCG provides efficient protection against severe and disseminated TB, such as tuberculosis meningitis and miliary TB, in children (33, 34, 40). However, its efficacy at preventing pulmonary TB in adults is controversial. Aronson et al. reported that BCG vaccination had long-term efficacy for American Indians and Alaskan natives (3), suggesting that a single dose offered protection for 50 to 60 years. The long-term efficacy estimates from clinical trials, observational case-control studies, and contact studies range from 0 to 80% (7), although the efficacy for the elderly is unknown. In the present study, we demonstrated that revaccination of elderly guinea pigs with BCG-Tokyo reduced bacterial replication in the lungs, alveolar lymph nodes, and spleen. In addition, in 60-month-old guinea pigs, PPD-specific IFN-γ responses were observed after the BCG-Tokyo booster vaccination. These findings suggest that BCG-Tokyo has a protective effect at all ages.

However, the efficacy of BCG revaccination is a matter of international debate (5). Several studies have shown that BCG revaccination had no protective efficacy against TB (19, 28, 32). Fjällbrant et al. reported that both primary vaccination and revaccination of tuberculin skin test-negative young adults caused a significant increase in the T-helper type 1 (Th1) immune response (12), a result consistent with the present findings in the old guinea pig model. This result suggests that BCG revaccination has a protective effect against TB. However, other factors that determine the efficacy of BCG revaccination, including age, duration of vaccination, and the influence of environmental mycobacteria, must be considered.

Cell-mediated immune responses play an essential role in the control of *M. tuberculosis* infection and TB. In particular, $CD4^+$ and $CD8^+$ T-cell subsets are considered to play important roles in the production of cytokines such as IFN-γ and tumor necrosis factor alpha (TNF-α). These cytokines are involved in inflammatory processes, including macrophage activation, control of *M. tuberculosis* replication, and granuloma formation (1, 10, 13). Using guinea pig models, Jeevan et al. suggested that BCG vaccination induces upregulation of IFN-γ and TNF-α after *M. tuberculosis* challenge (16). In the present study, we investigated IFN-γ responses by using an ELISPOT assay. To the best of our knowledge, this is the first study that used a guinea pig model together with an antigen-specific ELISPOT assay to show that BCG induces PPD-stimulated IFN-γ responses. The secretion of PPD-specific IFN-γ was observed in both young and old BCG-vaccinated guinea pigs. The number of PPD-specific IFN-γ-secreting cells was greater in 60-month-old vaccinated guinea pigs (group 1) than in young vaccinated guinea pigs (group 4). Because this was the second BCG vaccination for group 1, a booster effect may have occurred. Bacterial growth in the lungs, lymph nodes, and spleen was higher in unvaccinated guinea pigs (group 5) than in the vaccinated groups. The number of PPD-specific IFN-γ-producing PBMCs in the unvaccinated guinea pigs was significantly lower than that in the vaccinated guinea pigs. The results of our *M. tuberculosis* aerosol infection experiment suggest that the number of PPD-specific IFN-γ-producing PBMCs correlates with the level of protection against *M. tuberculosis*. While TNF-α is another important cytokine that protects against *M. tuberculosis*, BCG vaccination appears to modulate the potentially harmful effects of TNF-α and to reduce *M. tuberculosis* replication (26, 42). Recent studies have shown that general immune responses are important for resistance to *M. tuberculosis*. Interleukin-12 (IL-12) is required for dendritic cell migration (22), maintenance of pulmonary Th1 cells (11), and macrophage activation and subsequent production of IFN-γ. IL-27 has both proinflammatory and anti-inflammatory properties. IL-12 and/or *M. tuberculosis*-induced IL-27 gene expression in human macrophages may regulate macrophage function during *M. tuberculosis* infection (31). In addition, the importance of Th17 responses, including IL-17 and IL-23, in the pathophysiology of *M. tuberculosis* infection has been reported recently (4, 20, 21). *M. tuberculosis*-specific Th1 (IL-12 and IFN-γ) and Th17 responses play roles in the increased expression of cytotoxic T lymphocyte antigen 4 (CTLA-4) and programmed death-1 (PD-1), while IL-23 induces IFN-γ and supports the IL-17 response in the lungs. McMurray and colleagues, using a laser capture microdissection (LCM) technique, reported cytokine mRNA responses *in situ* in the pulmonary granulomas of nonvaccinated and BCG-vaccinated guinea pigs (23, 24). TNF-α mRNA was dominant in primary lesions microdissected from nonvaccinated guinea pigs at both 3 and 6 weeks postinfection, while the cytokine profiles of granulomas from BCG-vaccinated guinea pigs shifted from type 1 cytokine mRNA (IFN-γ and IL-12p40) at 3 weeks to a predominantly anti-inflammatory profile dominated by transforming growth factor-β (TGF-β) at 6 weeks (23, 24). These results suggest that BCG vaccination modulates cytokine responses in the lungs to promote antimycobacterial functions while controlling the potentially damaging inflammatory response.

A DTH skin test for PPD has been employed in the diagnosis of TB. While the test is highly sensitive for PPD, its specificity in the diagnosis of TB infection is controversial, because after BCG vaccination, a DTH response is detected. In the present study, DTH responses to PPD were detected in all of the guinea pigs vaccinated with BCG, and no significant difference was observed among the age groups. However, IFN-γ production by PBMCs was significantly different between the groups, and the number of PPD-specific IFN-γ-producing PBMCs correlated with the degree of protection against *M. tuberculosis*. These results suggest that ELISPOT assays that detect TB-specific immune responses may be the most accurate means of monitoring immunity against TB.

In Japan, individuals 65 years old or older represented 22.1% of the population in 2008, and this age group is expected to grow to one-third of the population by 2035 (8). This trend is seen in other countries as well. Currently, in Japan, more than 50% of the new cases of TB occur in patients ≥60 years old (29). The increasing susceptibility of the elderly to *M. tuberculosis* is generally thought to be associated with immune senescence, the most significant change being the loss or delayed production of antigen-specific $CD4^+$ T cells (14). In mice, an inadequate antigen-specific $CD4^+$ T-cell response is thought to contribute to increased susceptibility to *M. tuberculosis* infection (27). However, the mouse model has revealed that old mice express early resistance to pulmonary tuberculo-

sis infection (9, 39). $CD8^+$ T cells contribute to TB resistance via IL-12p70-dependent production of IFN-γ (35–38). However, this innate immune response is antigen independent, and the early resistance cannot be sustained. The bacterial load in the lungs of old mice increases about 90 days after infection (9), and the lungs of old mice are eventually more susceptible to bacterial growth (39). In the present study, antigen-specific IFN-γ production was observed after BCG revaccination of 60-month-old guinea pigs. In humans, the elderly have more preexisting diseases, such as diabetes mellitus (DM) and hypertension, some of which may be associated with an increased risk of TB (17). Clearly, further evaluation of BCG in the elderly is necessary.

In conclusion, we found that vaccination of elderly guinea pigs with BCG-Tokyo reduces bacterial replication in the lungs, alveolar lymph nodes, and spleens of infected animals. In addition, PPD-specific IFN-γ responses were observed after the second BCG-Tokyo vaccination. These findings suggest that BCG-Tokyo has a protective effect at all ages.

ACKNOWLEDGMENTS

We thank E. H. Jego and J. Khoh (Office of Medical Education, Nihon University School of Medicine) for revising the English of the manuscript.

REFERENCES

1. **Aktas, E., F. Ciftci, S. Bilgic, O. Sezer, E. Bozkanat, O. Deniz, U. Citici, and G. Deniz.** 2009. Peripheral immune response in pulmonary tuberculosis. Scand. J. Immunol. **70:**300–308.
2. **Andersen, P.** 2007. Tuberculosis vaccines—an update. Nat. Rev. Microbiol. **5:**484–487.
3. **Aronson, N. E., M. Santosham, G. W. Comstock, R. S. Howard, L. H. Moulton, E. R. Rhoades, and L. H. Harrison.** 2004. Long-term efficacy of BCG vaccine in American Indians and Alaska Natives: a 60-year follow-up study. JAMA **291:**2086–2091.
4. **Babu, S., S. Q. Bhat, N. P. Kumar, S. Jayantasri, S. Rukmani, P. Kumaran, P. G. Gopi, C. Kolappan, V. Kumaraswami, and T. B. Nutman.** 2009. Human type 1 and 17 responses in latent tuberculosis are modulated by coincident filarial infection through cytotoxic T lymphocyte antigen-4 and programmed death-1. J. Infect. Dis. **200:**288–298.
5. **Barreto, M. L., S. M. Pereira, and A. A. Ferreira.** 2006. BCG vaccine: efficacy and indications for vaccination and revaccination. J. Pediatr. (Rio J.) **82:** S45–S54.
6. **Black, G. F., R. E. Weir, S. Floyd, L. Bliss, D. K. Warndorff, A. C. Crampin, B. Ngwira, L. Sichali, B. Nazareth, J. M. Blackwell, K. Branson, S. D. Chaguluka, L. Donovan, E. Jarman, E. King, P. E. Fine, and H. M. Dockrell.** 2002. BCG-induced increase in interferon-gamma response to mycobacterial antigens and efficacy of BCG vaccination in Malawi and the UK: two randomised controlled studies. Lancet **359:**1393–1401.
7. **Brewer, T. F.** 2000. Preventing tuberculosis with bacillus Calmette-Guerin vaccine: a meta-analysis of the literature. Clin. Infect. Dis. **31**(Suppl 3)**:**S64–S67.
8. **Cabinet Office, Government of Japan.** 2008. Annual report on the aging society. http://www8.cao.go.jp/kourei/english/annualreport/index-wh.html.
9. **Cooper, A. M., J. E. Callahan, J. P. Griffin, A. D. Roberts, and I. M. Orme.** 1995. Old mice are able to control low-dose aerogenic infections with Mycobacterium tuberculosis. Infect. Immun. **63:**3259–3265.
10. **Cooper, A. M., and S. A. Khader.** 2008. The role of cytokines in the initiation, expansion, and control of cellular immunity to tuberculosis. Immunol. Rev. **226:**191–204.
11. **Feng, C. G., D. Jankovic, M. Kullberg, A. Cheever, C. A. Scanga, S. Hieny, P. Caspar, G. S. Yap, and A. Sher.** 2005. Maintenance of pulmonary Th1 effector function in chronic tuberculosis requires persistent IL-12 production. J. Immunol. **174:**4185–4192.
12. **Fjällbrant, H., M. Ridell, and L. O. Larsson.** 2007. Primary vaccination and revaccination of young adults with BCG: a study using immunological markers. Scand. J. Infect. Dis. **39:**792–798.
13. **Flynn, J. L., J. Chan, K. J. Triebold, D. K. Dalton, T. A. Stewart, and B. R. Bloom.** 1993. An essential role for interferon gamma in resistance to Mycobacterium tuberculosis infection. J. Exp. Med. **178:**2249–2254.
14. **Friedman, A., J. Turner, and B. Szomolay.** 2008. A model on the influence of age on immunity to infection with Mycobacterium tuberculosis. Exp. Gerontol. **43:**275–285.
15. **Gupta, U. D., and V. M. Katoch.** 2005. Animal models of tuberculosis. Tuberculosis (Edinb.) **85:**277–293.
16. **Jeevan, A., T. Yoshimura, K. E. Lee, and D. N. McMurray.** 2003. Differential expression of gamma interferon mRNA induced by attenuated and virulent Mycobacterium tuberculosis in guinea pig cells after Mycobacterium bovis BCG vaccination. Infect. Immun. **71:**354–364.
17. **Jeon, C. Y., and M. B. Murray.** 2008. Diabetes mellitus increases the risk of active tuberculosis: a systematic review of 13 observational studies. PLoS Med. **5:**e152.
18. **Kanekiyo, M., K. Matsuo, M. Hamatake, T. Hamano, T. Ohsu, S. Matsumoto, T. Yamada, S. Yamazaki, A. Hasegawa, N. Yamamoto, and M. Honda.** 2005. Mycobacterial codon optimization enhances antigen expression and virus-specific immune responses in recombinant Mycobacterium bovis bacille Calmette-Guérin expressing human immunodeficiency virus type 1 Gag. J. Virol. **79:**8716–8723.
19. **Karonga Prevention Trial Group.** 1996. Randomised controlled trial of single BCG, repeated BCG, or combined BCG and killed Mycobacterium leprae vaccine for prevention of leprosy and tuberculosis in Malawi. Lancet **348:**17–24.
20. **Khader, S. A., G. K. Bell, J. E. Pearl, J. J. Fountain, J. Rangel-Moreno, G. E. Cilley, F. Shen, S. M. Eaton, S. L. Gaffen, S. L. Swain, R. M. Locksley, L. Haynes, T. D. Randall, and A. M. Cooper.** 2007. IL-23 and IL-17 in the establishment of protective pulmonary $CD4^+$ T cell responses after vaccination and during Mycobacterium tuberculosis challenge. Nat. Immunol. **8:**369–377.
21. **Khader, S. A., and A. M. Cooper.** 2008. IL-23 and IL-17 in tuberculosis. Cytokine **41:**79–83.
22. **Khader, S. A., S. Partida-Sanchez, G. Bell, D. M. Jelley-Gibbs, S. Swain, J. E. Pearl, N. Ghilardi, F. J. Desauvage, F. E. Lund, and A. M. Cooper.** 2006. Interleukin 12p40 is required for dendritic cell migration and T cell priming after Mycobacterium tuberculosis infection. J. Exp. Med. **203:**1805–1815.
23. **Ly, L. H., M. I. Russell, and D. N. McMurray.** 2008. Cytokine profiles in primary and secondary pulmonary granulomas of guinea pigs with tuberculosis. Am. J. Respir. Cell Mol. Biol. **38:**455–462.
24. **Ly, L. H., M. I. Russell, and D. N. McMurray.** 2007. Microdissection of the cytokine milieu of pulmonary granulomas from tuberculous guinea pigs. Cell. Microbiol. **9:**1127–1136.
25. **McMurray, D. N.** 2001. Disease model: pulmonary tuberculosis. Trends Mol. Med. **7:**135–137.
26. **McMurray, D. N., S. S. Allen, A. Jeevan, T. Lasco, H. Cho, T. Skwor, T. Yamamoto, C. McFarland, and T. Yoshimura.** 2005. Vaccine-induced cytokine responses in a guinea pig model of pulmonary tuberculosis. Tuberculosis (Edinb.) **85:**295–301.
27. **Orme, I. M., J. P. Griffin, A. D. Roberts, and D. N. Ernst.** 1993. Evidence for a defective accumulation of protective T cells in old mice infected with Mycobacterium tuberculosis. Cell. Immunol. **147:**222–229.
28. **Rahman, M., M. Sekimoto, K. Hira, H. Koyama, Y. Imanaka, and T. Fukui.** 2002. Is bacillus Calmette-Guérin revaccination necessary for Japanese children? Prev. Med. **35:**70–77.
29. **Research Institute of Tuberculosis/JATA, Tuberculosis Surveillance Center.** 2009. Annual reports 2008. http://jata.or.jp/rit/ekigaku/en/index.php?annual%20report.
30. **Ritz, N., W. A. Hanekom, R. Robins-Browne, W. J. Britton, and N. Curtis.** 2008. Influence of BCG vaccine strain on the immune response and protection against tuberculosis. FEMS Microbiol. Rev. **32:**821–841.
31. **Robinson, C. M., and G. J. Nau.** 2008. Interleukin-12 and interleukin-27 regulate macrophage control of Mycobacterium tuberculosis. J. Infect. Dis. **198:**359–366.
32. **Rodrigues, L. C., S. M. Pereira, S. S. Cunha, B. Genser, M. Y. Ichihara, S. C. de Brito, M. A. Hijjar, I. Dourado, A. A. Cruz, C. Sant'Anna, A. L. Bierrenbach, and M. L. Barreto.** 2005. Effect of BCG revaccination on incidence of tuberculosis in school-aged children in Brazil: the BCG-REVAC cluster-randomised trial. Lancet **366:**1290–1295.
33. **Soysal, A., K. A. Millington, M. Bakir, D. Dosanjh, Y. Aslan, J. J. Deeks, S. Efe, I. Staveley, K. Ewer, and A. Lalvani.** 2005. Effect of BCG vaccination on risk of Mycobacterium tuberculosis infection in children with household tuberculosis contact: a prospective community-based study. Lancet **366:**1443–1451.
34. **Trunz, B. B., P. Fine, and C. Dye.** 2006. Effect of BCG vaccination on childhood tuberculous meningitis and miliary tuberculosis worldwide: a meta-analysis and assessment of cost-effectiveness. Lancet **367:**1173–1180.
35. **Turner, J., A. A. Frank, and I. M. Orme.** 2002. Old mice express a transient early resistance to pulmonary tuberculosis that is mediated by CD8 T cells. Infect. Immun. **70:**4628–4637.
36. **Vesosky, B., D. K. Flaherty, E. K. Rottinghaus, G. L. Beamer, and J. Turner.** 2006. Age dependent increase in early resistance of mice to Mycobacterium tuberculosis is associated with an increase in CD8 T cells that are capable of antigen independent IFN-γ production. Exp. Gerontol. **41:**1185–1194.
37. **Vesosky, B., D. K. Flaherty, and J. Turner.** 2006. Th1 cytokines facilitate CD8-T-cell-mediated early resistance to infection with Mycobacterium tuberculosis in old mice. Infect. Immun. **74:**3314–3324.
38. **Vesosky, B., E. K. Rottinghaus, C. Davis, and J. Turner.** 2009. CD8 T cells

in old mice contribute to the innate immune response to Mycobacterium tuberculosis via interleukin-12p70-dependent and antigen-independent production of gamma interferon. Infect. Immun. **77:**3355–3363.

39. **Vesosky, B., and J. Turner.** 2005. The influence of age on immunity to infection with Mycobacterium tuberculosis. Immunol. Rev. **205:**229–243.
40. **Walker, V., G. Selby, and I. Wacogne.** 2006. Does neonatal BCG vaccination protect against tuberculous meningitis? Arch. Dis. Child. **91:**789–791.
41. **Yamamoto, S., and T. Yamamoto.** 2007. Historical review of BCG vaccine in Japan. Jpn. J. Infect. Dis. **60:**331–336.
42. **Yamamoto, T., T. M. Lasco, K. Uchida, Y. Goto, A. Jeevan, C. McFarland, L. Ly, S. Yamamoto, and D. N. McMurray.** 2007. Mycobacterium bovis BCG vaccination modulates TNF-α production after pulmonary challenge with virulent Mycobacterium tuberculosis in guinea pigs. Tuberculosis (Edinb.) **87:**155–165.

Vaccine 28 (2010) 4616–4625

Contents lists available at ScienceDirect

Vaccine

journal homepage: www.elsevier.com/locate/vaccine

Identification of murine T-cell epitopes on low-molecular-mass secretory proteins (CFP11, CFP17, and TB18.5) of *Mycobacterium tuberculosis*

Ghada Eweda[a], Daisuke Suzuki[b], Toshi Nagata[c,*], Kunio Tsujimura[a], Yukio Koide[a]

[a] Department of Infectious Diseases, Hamamatsu University School of Medicine, 1-20-1 Higashi-ku, Handa-yama, Hamamatsu 431-3192, Japan
[b] 3rd Department of Internal Medicine, Hamamatsu University School of Medicine, 1-20-1 Higashi-ku, Handa-yama, Hamamatsu 431-3192, Japan
[c] Department of Health Science, Hamamatsu University School of Medicine, 1-20-1 Higashi-ku, Handa-yama, Hamamatsu 431-3192, Japan

ARTICLE INFO

Article history:
Received 25 December 2009
Received in revised form 23 April 2010
Accepted 26 April 2010
Available online 8 May 2010

Keywords:
Mycobacterium tuberculosis
T-cell epitopes
Low-molecular-mass proteins

ABSTRACT

The low-molecular-mass secretory proteins of *Mycobacterium tuberculosis* have been shown to be major T-cell antigens during infection with the pathogenic bacterium. In this study, we determined murine T-cell epitopes on three low-molecular-mass proteins, CFP11 (Rv2433c), CFP17 (Rv1827), and TB18.5 (Rv0164) using DNA immunization of inbred mice. We analyzed interferon-γ production from immune splenocytes in response to overlapping peptides covering these proteins. We identified two CD8+ T-cell epitopes on CFP11 and CFP17, one in BALB/c mice and the other in C57BL/6 mice, respectively. On TB18.5, we identified a CD8+ T-cell epitope in BALB/c mice and a CD4+ T-cell epitope in C57BL/6 mice. With the aid of computer algorithms, we could identify the minimal CD8+ T-cell epitopes. These T-cell epitopes are feasible for analysis of the role of antigen-specific T cells during *M. tuberculosis* infection.

1. Introduction

According to the latest tuberculosis (TB) global burden estimates, there were 9.27 million incident cases of TB in 2007 with approximately one third of the total world population being infected [1]. To date, *Mycobacterium bovis* bacillus Calmette-Guérin (BCG) is the only approved vaccine against TB [2,3]. Despite the fact that BCG is among the most widely used vaccines throughout the world, TB still poses a serious threat to global health. Whereas BCG is believed to protect newborn and young children against early manifestations of TB, its efficacy against pulmonary TB in adults is still a subject of debate [4], and has been reported to wane with time since vaccination [5]. Variable levels of protective efficacy ranging from 0% to 80% have been reported in different studies [2,4]. Moreover, the viable nature of BCG makes it partly unsafe in cases of immunocompromised individuals. This highlights a need to develop a more effective, safe and reliable vaccine against TB [6].

A T-cell mediated immune response is critical for the development of resistance against mycobacterial infection [7,8]. It has been well established that major histocompatibility complex (MHC) class II-restricted CD4+ T cells are important mediators of host defense against TB. In addition, MHC class I-restricted CD8+ T cells have also been reported to be required for the optimum control of mycobacterial infection [9,10].

An essential step towards the development of a new vaccine against TB is gaining more information on the antigenic architecture of *Mycobacterium tuberculosis* to identify T-cell epitopes responsible for eliciting protective immune responses [6,11]. Determination of the complete genome sequence of *M. tuberculosis* facilitated this step considerably [12]. The observation that only immunization with live *M. tuberculosis* can induce effective protective T-cell responses [13] has drawn great attention to the study of proteins that are actively secreted into the culture medium by the replicating organism due to their potential immunogenic role.

M. tuberculosis culture fluid proteins (CFPs) have been shown to be of particular relevance as protective T-cell antigens [14–16]. Especially, relatively low-molecular-mass polypeptides (less than 20 kDa) in CFPs have been reported to be major antigens that evoke T-cell responses [17,18]. ESAT-6 and CFP10 proteins are widely used these days in whole blood interferon (IFN)-γ release assays for TB diagnosis [19]. CFP17 was purified using two-dimensional electrophoresis and identified as a T-cell antigen using the mouse system reported by Weldingh and co-workers [20,21]. In their study, CFP17 was demonstrated as one of the most potent inducers of IFN-γ release among the investigated CFPs in *M. tuberculosis*-immune mice. TB18.5 was reported in a study by Lim et al. [22], using peripheral blood mononuclear cells from healthy tuberculin reactors, to be a T-cell-stimulating antigen in humans. In that study, CFP17 and TB18.5 were described as MTSP14 and MTSP17, respectively. CFP11, CFP17, and TB18.5 were identified as human immunodominant T-cell antigens in a study by Sable et al. [23]

* Corresponding author. Tel.: +81 53 435 2332; fax: +81 53 435 2332/2335.
E-mail address: tnagata@hama-med.ac.jp (T. Nagata).

0264-410X/$ – see front matter © 2010 Elsevier Ltd. All rights reserved.
doi:10.1016/j.vaccine.2010.04.079

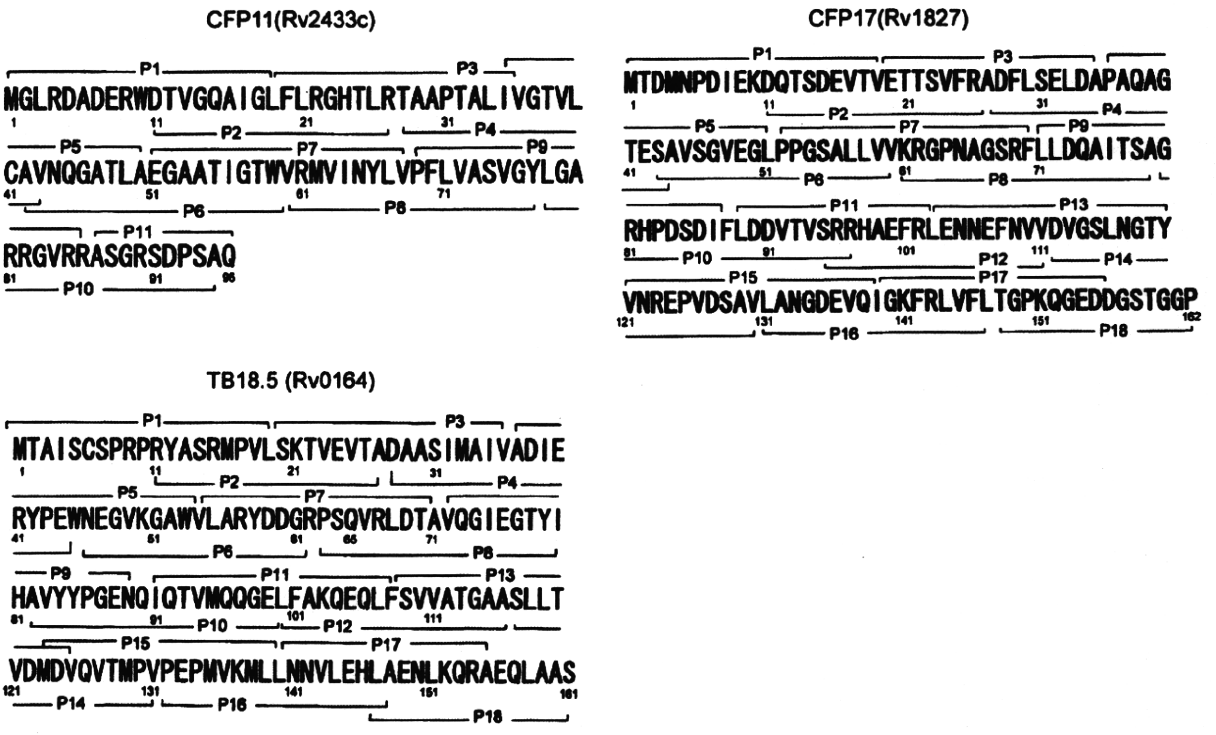

Fig. 1. Schematic representation of overlapping synthetic peptides of CFP11, CFP17, and TB18.5 proteins of *M. tuberculosis*. All peptides covering entire CFP11 (Rv2433c), CFP17 (Rv1827), and TB18.5 (Rv0164) proteins of *M. tuberculosis* were synthesized as approximately 20-mer molecules overlapping by approximately 10 amino acids.

using human peripheral blood and pleural fluid mononuclear cells. In that study, CFP11, which was described as one of the newly identified T-cell antigens, was reported to induce marked increase in serum IgG levels as well as IFN-γ production and lymphocyte proliferation. In the same study, TB18.5 was in the top 10 out of 104 polypeptides that induced prominent T-cell responses based on IFN-γ production and lymphocyte proliferation. These proteins were purified from the culture filtrate of *M. tuberculosis*, but they were also found in the cell wall fraction following two-dimensional electrophoresis analysis [24]. The structure of CFP11 has been elucidated by de novo methods [25].

DNA immunization with gene gun bombardment is a reliable method to induce reproducible T-cell responses [26], and has been used for the identification of T-cell epitopes of *M. tuberculosis* antigens including antigen (Ag) 85 family proteins (Ag85A, Ag85B, and Ag85C) [27,28] and MPT51 [29,30]. Here, we identified murine T-cell epitopes on three low-molecular-mass secretory proteins, CFP11 (Rv2433c), CFP17 (Rv1827), and TB18.5 (Rv0164) using gene gun immunization of inbred mice with plasmid DNA, restimulation with overlapping synthetic peptides spanning the entire amino acid (aa) sequences, and MHC binding peptide prediction algorithms for the prediction of minimal T-cell epitopes.

2. Materials and methods

2.1. Animals

BALB/c and C57BL/6 mice (Japan SLC; Hamamatsu, Japan) were maintained in the Animal Facility at Hamamatsu University School of Medicine. Mice between 2 and 4 months of age were used for immunization. All animal experiments were performed according to the Guidelines for Animal Experimentation, Hamamatsu University School of Medicine.

2.2. Plasmid construction

DNAs encoding CFP11, CFP17, and TB18.5 were amplified from *M. tuberculosis* H37Rv genome by PCR. Primers used for PCR are as follows: 5′-CGAGAATTCACCATGGGCCTGCGCGACG-3′ and 5′-ATAGTTTAGCGGCCGCACCGTCATTGTGCTGATGG-3′ for CFP11, 5′-CGACTCGAGCACCATGACGGACATGAACCCGG-3′ and 5′-ATAGTTTAGCGGCCGCTCACGGGCCCCC-3′ for CFP17, and 5′-CGAGAATTCACCATGACGGCAATCTCGTGC-3′ and 5′-ATAGTTTAGCGGCCGCTTAGCTGGCCGCGAC-3′ for TB18.5 (the underlined portions indicate restriction enzyme recognition sequences.) The PCR fragments were inserted between EcoRI and Not I sites for CFP11 and TB18.5, and between Xho I and Not I for CFP17, located downstream of cytomegalovirus immediate-early enhancer/promoter region of eukaryotic expression plasmid, pCI (Promega, Madison, WI, USA), resulting in pCI-CFP11, pCI-CFP17, and pCI-TB18.5, respectively. The integrity of the nucleotide sequence was validated by automated DNA sequencing with an ABI PRISM 310 genetic analyzer (Applied Biosystems, Foster City, CA, USA) using a Dye Primer Cycle Sequencing kit (Applied Biosystems). The aa sequences of CFP11, CFP17, and TB18.5 are identical in *M. tuberculosis* and *M. bovis* (Fig. 1). CFP11 aa sequences are NP_216949 (NCBI reference number) for *M. tuberculosis*, NP_856106 (NCBI) for *M. bovis*; CFP17 aa sequences are CAB01474 (GenBank reference number) for *M. tuberculosis*, CAD94561 (GenBank) for *M. bovis*; and TB18.5 aa sequences are YP_177617 (NCBI) for *M. tuberculosis*, CAD93033 (GenBank) for *M. bovis*.

2.3. Immunization

Helios gene gun system (Bio-Rad Laboratories, Hercules, CA, USA) was used for DNA immunization. Preparation of a DNA-coated gold particle cartridge was performed according to the manufacturer's instructions. Finally, 0.5 mg of gold particles was coated with